

Five Amino Acids in the Innermost Cavity of the Substrate Binding Cleft of Organic Cation Transporter 1 Interact with Extracellular and Intracellular Corticosterone¹

Christopher Volk, Valentin Gorboulev, Alexander Kotsch, Thomas D. Müller, and Hermann Koepsell

Institute of Anatomy and Cell Biology (C.V., V.G., H.K.) and Department of Molecular Plant Physiology and Biophysics, Julius-von-Sachs Institute (A.K., T.D.M), Universität Würzburg, Würzburg, Germany

Running title: Outward- and Inward-facing Substrate Binding Sites of rOCT1

Address correspondence to: Hermann Koepsell or Christopher Volk, Institute of Anatomy and Cell Biology, Koellikerstr. 6, 97070 Würzburg, Germany, E-mail:

Hermann@Koepsell.de, C.Volk@mail.uni-wuerzburg.de

Number of text pages: 29

Number of tables: 3

Number of figures: 12

Number of references: 26

Number of words in abstract: 249

Number of words in introduction: 682

Number of words in discussion: 2123

ABBREVIATIONS: OCT, organic cation transporter; TMH, transmembrane helix; LacY, lactose permease from *Escherichia coli*; TEA⁺, tetraethylammonium; MPP⁺, 1-methyl-4-phenylpyridinium; TBuA⁺, tetrabutylammonium; PCR, polymerase chain reaction, HEK, human embryonic kidney.

ABSTRACT

Previously we showed that Leu447 and Gln448 in the transmembrane helix (TMH) 10 of rat organic cation transporter rOCT1 are critical for inhibition of cation uptake by corticosterone. Here, we tested whether the affinity of corticosterone is different when applied from the extracellular or intracellular side. The affinity of corticosterone was determined by measuring the inhibition of currents induced by tetraethylammonium⁺ (TEA⁺) in *Xenopus laevis* oocytes expressing rOCT1. Either corticosterone and TEA⁺ were added to the bath simultaneously, or the oocytes were preincubated with corticosterone, washed, and TEA⁺-induced currents were determined subsequently. In mutant Leu447Tyr, K_i values for extracellular and intracellular corticosterone were decreased whereas in mutant Gln448Glu only the K_i for intracellular corticosterone was changed. Modelling of the interaction of corticosterone with rOCT1 in the inward- or outward-facing conformation predicted direct binding to Leu447, Phe160 (TMH2), Trp218 (TMH4), Arg440 (TMH10), and Asp475 (TM11) from both sides. In mutant Phe160Ala, affinities for extracellular and intracellular corticosterone were increased whereas maximal inhibition was reduced in Trp218Phe and Arg440Lys. In stably transfected epithelial cells, the affinities for inhibition of 1-methyl-4-phenylpyridinium⁺ (MPP⁺) uptake by extracellular and intracellular corticosterone were decreased when Asp475 was replaced by glutamate. In mutants Phe160Ala, Trp218Tyr, Arg440Lys and Leu447Phe the affinities for MPP⁺ uptake, and in mutant Asp475Glu the affinity for TEA⁺ uptake were changed. The data suggest that Phe160, Trp218, Arg440, Leu447 and Asp475 are located within an innermost cavity of the binding cleft that is alternatingly exposed to the extracellular or intracellular side during substrate transport.

Polyspecific organic cation transporters (OCTs) of the *SLC22* family play important roles in the elimination, distribution and homeostasis of drugs. In addition they are involved in the re-uptake of neurotransmitters into neurons and release of acetylcholine during non-neuronal cholinergic reactions (Koepsell et al., 2007; Lips et al., 2005; Reitman and Schadt, 2007). Three OCT subtypes with overlapping substrate specificities and tissue distributions have been identified (Koepsell et al., 2007). OCT1, OCT2 and OCT3 are polyspecific facilitated diffusion systems that are able to translocate organic cations in both directions across the plasma membrane. However, it is so far unclear how OCTs recognize substrates and inhibitors exhibiting different chemical structures and how substrate translocation is achieved. Extensive mutagenesis experiments performed in rat OCT1 (rOCT1) revealed that seven amino acids localized in the 4th, 10th and 11th transmembrane helix (TMH) are critical for substrate and inhibitor specificity (Gorboulev et al., 1999; Gorboulev et al., 2005; Popp et al., 2005). Modelling of the rOCT1 structures using the inward-facing structure of lactose permease (LacY) from *Escherichia coli* (Abramson et al., 2003; Popp et al., 2005), suggested that the residues critical for substrate affinity are localized within a large inward-open cleft and are accessible from the solvent space. In analogy to the conformational changes of the permease LacY via the alternating access mechanism model - which has been experimentally demonstrated for LacY (Kaback et al., 2007; Majumdar et al., 2007; Smirnova et al., 2006) - we have also modelled the outward-facing conformation of rOCT1 with the binding cleft opened to the extracellular space (Gorbunov et al., 2008). So far, two observations support the hypothesis that OCTs operate via an alternating access mechanism model similar to LacY. Firstly, measuring interactions of nontransported inhibitors applied from the extracellular or intracellular side of the plasma membrane provide evidence that the substrate binding region of rat OCT2 (rOCT2)

is accessible from the extracellular and intracellular side (Volk et al., 2003). Secondly, we demonstrated that mutations in modelled contact regions between TMH2 and TMH11, which interact in the inward-facing model and are detached in the outward-facing model, may partially inhibit transport activity (Gorbunov et al., 2008).

Recently we identified two residues that are responsible for increased affinity of corticosterone to inhibit uptake of tetraethylammonium⁺ (TEA⁺) by rOCT2 compared to rOCT1 (Gorboulev et al., 2005). Upon replacement of Leu447 and Gln448 in TMH10 of rOCT1 by the corresponding amino acids of rOCT2 (mutant rOCT1(L447Y,Q448E)), the IC₅₀ value for inhibition of [¹⁴C]TEA⁺ uptake by corticosterone decreased to the value observed in rOCT2. The Michaelis Menten constant (K_m) for 1-methyl-4-phenylpyridinium⁺ (MPP⁺) uptake was also decreased in rOCT1(L447Y,Q448E) suggesting that Leu447 and/or Gln448 are/is located within the substrate binding region. The K_i values for corticosterone-mediated inhibition of TEA⁺ uptake were determined using an incubation time of 30 min. Since corticosterone permeates the plasma membrane passively during this time period (Arndt et al., 2001), we cannot distinguish whether the mutations increase the affinity for corticosterone from the extracellular, from the intracellular, or from both sides of the plasma membrane.

The structure models of the inward-facing and outward-facing conformations of rOCT1 (Gorbunov et al., 2008; Popp et al., 2005) suggested that Leu447 may contribute to the outward- and inward-facing cleft whereas Gln448 seemed only be accessible in the inward open cleft. To determine whether residues that contribute to both, the outward-facing and the inward-facing substrate binding region can be identified experimentally, we investigated if the mutations Leu447Tyr and Gln448Glu alter the affinity for corticosterone, which was applied to the

extracellular or intracellular side of the plasma membrane. From docking analysis of corticosterone in the outward-facing and inward-facing binding clefts of rOCT1 we could identify additional amino acids that possibly interact with corticosterone and were thus tested by mutagenesis.

Here we present evidence that the residues Phe160 (TMH2), Trp218 (TMH4), Arg440 (TMH10), Leu447 (TMH10) and Asp475 (TMH11) are located in the innermost cavities of the outward-facing as well as the inward-facing substrate binding clefts. All these residues participate in the binding of corticosterone on either side of the plasma membrane and are critical for the binding affinity of MPP⁺ or TEA⁺.

Material and Methods

Materials. [¹⁴C]TEA⁺ (1.9 GBq/mmol) and [³H]-1-methyl-4-phenylpyridinium⁺ (MPP⁺) (3.1 TBq/mmol) were obtained from Biotrend (Köln, Germany). All other chemicals were obtained as described earlier (Arndt et al., 2001; Volk et al., 2003)

Site-Directed-Mutagenesis. Point mutations were introduced into rOCT1 by polymerase chain reaction (PCR) applying the overlap extension method as described (Ho et al., 1989; Gorboulev et al. 2005; Popp et al. 2005). The cloned fragments were sequenced to confirm the presence of the desired mutations.

Expression of rOCT1 and Mutants in Oocytes of *Xenopus laevis*. *X. laevis* oocytes were prepared as described previously (Arndt et al., 2001) and stored in Ori buffer (5mM MOPS, 100mM NaCl, 3mM KCl, 2mM CaCl₂ and 1mM MgCl₂, adjusted to pH 7.4 using NaOH) supplemented with 50mg/l gentamycin. 10ng cRNA encoding for wildtype rOCT1 or the mutants were injected in a volume of 50nl H₂O into single oocytes. Oocytes were then stored for 3-5 days in Ori buffer at 16° C. Noninjected oocytes from the respective batch served as controls.

Electrophysiology. Two-electrode-voltage-clamp measurements were performed as described (Nagel et al., 1997; Volk et al., 2003). Oocytes were superfused continuously with Ori buffer at room temperature (~2ml/min) and routinely clamped to a holding potential of -50mV using a Warner OC 725 amplifier (Warner Instruments, Hamden, CT). Apparent K_m values for TEA⁺ were determined by superfusing voltage-clamped oocytes with increasing TEA⁺ concentrations and recording the induced inward currents.

Inhibition of TEA⁺-induced Currents by Tetrabutylammonium⁺ or Corticosterone. To measure the inhibition of TEA⁺-induced inward currents due to binding of tetrabutylammonium⁺ (TBuA⁺) or corticosterone to rOCT1 from the extracellular side, oocytes were superfused for 45s with Ori buffer containing TEA⁺, TEA⁺ plus TBuA⁺, or TEA⁺ plus corticosterone. The concentration dependence for inhibition of rOCT1 by TBuA⁺ or corticosterone was determined by starting the superfusion with the lowest inhibitor concentration. After each superfusion period, the oocytes were washed for 1min with Ori buffer. To measure inhibition of TEA⁺-induced inward currents due to corticosterone binding from the intracellular side, oocytes were clamped to -50mV, equilibrated for 10min with corticosterone and washed for 1min with Ori buffer. Then TEA⁺-induced inward currents were measured during a 45s superfusion period with TEA⁺. The 10min-equilibration periods in the presence of corticosterone were started at the lowest corticosterone concentration.

Control experiments showed that the cytosolic corticosterone concentration required for inhibition of rOCT1 from the intracellular side is reached after 10min of incubation (equilibration control) and that the access of corticosterone to the extracellular surface after 45s incubation with corticosterone from the extracellular side as well as 10min pre-incubation with corticosterone can be eliminated with a 1min-wash using Ori buffer (wash controls). The equilibration control was

performed with the mutant rOCT1(C451M, Q448E), which has a much higher affinity for corticosterone applied to the intracellular side as when applied from the extracellular side (Table 1). When oocytes expressing rOCT1(C451M, Q448E) were incubated for 10min or 30min with 4.6 μ M corticosterone virtually identical inward currents were obtained after superfusion with 0.2mM TEA⁺. The currents amounted to 52 \pm 4 % (10min incubation, n = 4) and 48 \pm 4 % (30min incubation, n = 4 each) of the currents obtained without corticosterone pre-treatment. Since 4.6 μ M corticosterone is the half maximal concentration (IC_{50(cort.)}) for inhibition of rOCT1(C451M, Q448E) from the intracellular side, and the IC_{50(cort.)} from extracellular is 10-fold higher, we conclude that the cytosolic concentration of corticosterone is equilibrated after 10min incubation. The wash controls were performed with rOCT1(C451M) which exhibits a higher affinity for corticosterone applied from extracellular than from the intracellular side (Table 1). In oocytes expressing rOCT1(C451M) current induced by superfusion with 0.2mM TEA⁺ was inhibited by 50 \pm 3 % (n = 4) when 45s superfusion with TEA⁺ was performed in the presence of 49 μ M corticosterone, a concentration that represents the IC_{50(cort.)} from extracellular. The inhibition was virtually abolished (2 \pm 2 %, n = 4) after the oocytes had been washed for 1min with Ori buffer indicating that extracellular corticosterone as well as corticosterone that had entered the plasma membrane during the 45s superfusion was removed. To demonstrate that intracellular corticosterone or corticosterone inside the plasma membrane does not get access to the extracellular side during electrical measurements of washed oocytes that had been preincubated with corticosterone, we incubated oocytes expressing rOCT1(C451M) for 10min with 49 μ M corticosterone, washed them for 1min with Ori buffer, and measured the current induced by superfusion with 0.2mM TEA⁺. The TEA⁺-induced current amounted to 15 \pm 3% (n = 4) of the current obtained

without corticosterone pre-treatment. Since this inhibition is due to inhibition from intracellular ($IC_{50(\text{cort.})}$ from intracellular = $132\mu\text{M}$, Table 1), we conclude that intracellular corticosterone or corticosterone within the plasma membrane does not get significant access to the extracellular side of the transporter.

Tracer uptake measurements. *Xenopus laevis* oocytes expressing rOCT1 were incubated for 15min at room temperature in Ori buffer containing [^{14}C]TEA⁺ in the presence of different concentrations of MPP⁺. Subsequently, the oocytes were washed three times with ice-cold Ori buffer, solubilized by using 5% SDS solution and the intracellular radioactivity was analyzed by liquid scintillation counting using a Packard TriCarb 1600 counter.

[^3H]MPP⁺ uptake into human embryonic kidney (HEK) 293 cells stably transfected with wildtype rOCT1 or rOCT1(D475E) was measured as described (Mehrens et al., 2000; Minuesa et al., 2009). Cells were detached from culture plates by incubation with Ca²⁺ and Mg²⁺ free PBS and suspended in PBS containing 0.5 mM MgCl₂ and 1 mM CaCl₂ (transport PBS). To measure inhibition of [^3H]MPP⁺ uptake by extracellular corticosterone, 90 μl of cells were placed at the bottom of 2ml tubes and incubated for 40s at 37°C. 10 μl of transport PBS containing 0.13 μM [^3H]MPP⁺ plus different concentrations of corticosterone were placed on the inner wall of the tube above the cell suspension. Uptake was started by vortexing the tube and stopped after 1s by adding 1ml of ice-cold transport PBS containing 100 μM quinine (stop solution). To measure inhibition of [^3H]MPP⁺ (0.013 μM) uptake by intracellular corticosterone, the cells were pre-incubated for 10min at 37°C in transport PBS containing different concentrations of corticosterone. 20 μl of the pre-incubated cells were placed at the inner walls of 2ml tubes that were pre-loaded with 300 μl of transport PBS (37°C) containing [^3H]MPP⁺ (0.013 μM). Uptake was started by vortexing and stopped by adding ice-

cold stop solution. Cells were spun down, washed with stop solution, solubilized with 4M guanidine thiocyanate, and analyzed for radioactivity by liquid scintillation counting. Performing control experiments with rOCT1 mutants with an about 10fold lower affinity for intracellular versus extracellular corticosterone we verified that the corticosterone concentration at the outward-facing transporter was reduced effectively when cells that were pre-incubated with corticosterone were diluted in transport buffer without corticosterone.

Simulation of the Interaction of Corticosterone and TBuA⁺ with rOCT1. The software of SYBYL version 7.1 (Tripos Inc, St. Louis, MO) including the force field software MMFF94s was used throughout the simulations. For docking of corticosterone a template coordinate set was obtained from the database (<http://ligand-depot.resb.org>), for TBuA⁺ the coordinates were obtained from the database Hic-up (<http://xray.bmc.uu.se/hicup>), hydrogen atoms were attached to all heavy atoms and the resulting structure was subsequently energy-minimized employing a conjugate gradient algorithm. Previously established homology models of the inward-facing and outward-facing conformations of rOCT1 were used for docking simulations. The inward-facing conformation was built on basis of the crystal structure of LacY (Abramson et al., 2003; Popp et al., 2005). A model of the outward-facing conformation of rOCT1 was constructed as described recently (Gorbunov et al., 2008). Basically, a rigid-body movement of the first six helices (N-terminal domain) with respect to the last six helices (C-terminal domain) was performed in analogy to the model proposed for LacY allowing some intrahelix motions and drifting of individual domains. For LacY this helix rearrangement has been proposed, modelled and demonstrated experimentally (Abramson et al., 2003; Ermolova et al., 2006; Holyoake and Sansom, 2007; Kaback et al., 2007; Smirnova et al., 2007). The structure models of the inward- and outward-facing conformations

of rOCT1 were complemented with hydrogens and partial charges were assigned using the AMBER7 FF02 force field.

Docking of corticosterone to the outward- and inward-facing conformation of rOCT1 and TBuA⁺ to the outward-facing conformation were performed using the FlexX module of Sybyl7.1 software (Tripos Inc., St. Louis, MO). For simulations, the side chains of lysine residues were protonated and the carboxylate groups of aspartic and glutamic acids were ionized whereas cysteine residues were treated as neutral. Flexible docking of corticosterone and TBuA⁺ was performed with FlexX (Rarey et al., 1996) selecting the place particles option (Rarey et al., 1999). Two rounds of simulations were performed. In the first rounds, docking hits of the corticosterone or TBuA⁺ molecule were accepted at any site in the interior cleft of the inward- and/or outward-facing conformations of OCT1 and the results were sorted according to their docking energies using the corresponding total FlexX-Scores (calculated free binding energy in kJ/mol). The docking simulations for corticosterone in the first round were consistent with our mutagenesis data showing that Leu447 is critical for the affinity of corticosterone in the outward-facing as well as in the inward-facing rOCT1 conformation. The majority of the docking results suggested an additional interaction of corticosterone with residues Phe160 and/or Tyr222. Additional mutagenesis experiments with these two residues revealed that the affinities of corticosterone to both, the outward-facing and inward-facing conformation of rOCT1 were increased when Phe160 was replaced by alanine whereas replacement of Tyr222 by phenylalanine did not change the affinity of corticosterone. We therefore performed a second docking simulation using more stringent docking site restraints around residues Leu447 and Phe160. A radius of 5Å around each of the residues was defined to allow docked molecules to be selected.

The docking simulations for TBuA⁺ to the outward-facing conformation in the first round indicated several putative interaction sites including a site close to Asp475. Since the affinity of TBuA⁺ to rOCT1 is increased when Asp475 is replaced by glutamate (Gorboulev et al., 1999) we performed a second round of simulation defining a radius of 6.5Å around Asp475 in which docking of TBuA⁺ was allowed.

Calculations and Statistics. All electrophysiological measurements were performed with oocytes from at least 3 different batches. IC₅₀ values for inhibition by corticosterone or TBuA⁺ of currents induced by superfusion with TEA⁺ were calculated by fitting the Hill equation allowing adjustment to different degrees of maximal inhibition. Fitting was performed to measurements with individual oocytes (for statistic comparison) and to compiled data sets (for figures). Competition between TEA⁺ and corticosterone or TBuA⁺ was tested by checking whether the IC₅₀ values measured at 0.2mM and 2mM TEA⁺ reveal the same K_i value when competition is assumed using equation 1.

$$(1) \quad K_{i(\text{compet.})} = \frac{\text{IC}_{50}}{1 + S / K_{m(\text{TEA})}}$$

S represents the employed concentration of TEA⁺ and K_{m(TEA)} the mean value of 75μM obtained for TEA⁺-induced currents in wildtype rOCT1 and employed mutants. Competitive inhibition predicts that the IC₅₀ values measured with 2mM and 0.2mM TEA⁺ are 28.4- and 3.74-times higher, respectively, than the calculated K_i value, and that IC₅₀ values measured with 2mM TEA⁺ are 7.59-times higher (f_(compet.)) compared to the values obtained with 0.2mM TEA⁺. In some experiments the observed factors between the IC₅₀ values at 2mM and 0.2 mM TEA⁺ were smaller indicating partial competition (f_(part. compet.)). In case of partial competition we

estimated the K_i values from the IC_{50} values measured with 0.2mM TEA⁺ according to equation 2:

$$(2) \quad K_{i(\text{part. compet.})} = \frac{IC_{50}}{1 + \frac{S \times f_{(\text{part. compet.})}}{K_{m(\text{TEA})} \times f_{(\text{compet.})}}$$

For example, when corticosterone was applied from the extracellular side of oocytes expressing rOCT1 wildtype, the IC_{50} value measured with 2mM TEA⁺ was 3.89-times higher than those measured with 0.2mM TEA⁺ ($f_{(\text{part. compet.})}$) and the K_i value was estimated by dividing the IC_{50} value by 2.37 (divider in equation 2).

In tracer uptake measurements with oocytes, uptake rates were calculated from 7-10 oocytes for each data point. Apparent K_m values for [³H]MPP⁺ uptake and $I_{(0.5\text{TEA})}$ values for activation of TEA⁺-induced currents were calculated by fitting the Michaelis-Menten equation to the data whereas IC_{50} values for inhibition of [¹⁴C]TEA⁺ uptake by MPP⁺ were calculated using the Hill equation. In the figures means of 4-10 individual experiments from at least three different batches of oocytes are presented. Measuring the inhibition of MPP⁺ uptake by corticosterone in HEK293 cells, seven corticosterone concentrations were tested in three independent experiments. In each experiment and data point four uptake measurements were performed. The IC_{50} values were determined by fitting the Hill equation to the data. Since 0.013 μM MPP⁺ is far below the K_m value for MPP⁺ the IC_{50} values are virtually identical to the K_i values

Data are presented as means ± S.E.M. One way ANOVA with post hoc Tukey test was employed to evaluate differences using Prism4.0 (GraphPad Software Inc., San Diego, CA). P values < 0.05 were considered to be statistically significant.

Results

The Mutation C451M in rOCT1 Increases TEA⁺-induced Currents but Does not Alter Affinity. [¹⁴C]TEA⁺ uptake measurements in oocytes expressing rOCT1 showed that the affinity of corticosterone was increased when Leu447 and Gln448 in TMH10 of rOCT1 were replaced by tyrosine or glutamic acid, respectively (Gorboulev et al., 2005). To determine whether these mutations alter the affinity of corticosterone from the extracellular side of the plasma membrane we measured short term effects of corticosterone on TEA⁺-induced currents. The currents after superfusion with 2mM TEA⁺ (-50mV) were 3-8 times smaller in the mutants compared to rOCT1 wildtype (Fig. 1A, currents: wildtype > L447Y > Q448E > L447Y,Q448E) and did not allow to determine reliable concentration inhibition curves. To overcome this technical obstacle we made use of our recent observation that I_{\max} values for cation-induced currents by rOCT1 are increased when Cys451 is replaced by methionine (Sturm et al., 2007), and introduced this point mutation in the mutants with increased sensitivity to corticosterone. Conformingly, TEA⁺-induced currents were increased as expected (Fig. 1A).

Previously we observed that the choline concentration inducing half maximal currents ($I_{0.5(\text{choline})}$) in rOCT1(C451M) was increased when Cys322 was replaced with serine, whereas the same mutation in wildtype background showed no effect (Sturm et al., 2007). To test for effects of rOCT1(C451M) background, we measured the half maximal concentrations for TEA⁺ currents ($I_{0.5(\text{TEA})}$) in oocytes expressing rOCT1, rOCT1(C451M), rOCT1(C451M,L447Y), rOCT1(C451M,Q448E), or rOCT1(C451M,L447Y,Q448E). Previous [¹⁴C]TEA⁺ uptake measurements showed that the apparent $K_{m(\text{TEA})}$ values as well as the K_i values for TEA⁺ inhibition of TEA⁺ uptake were not significantly different in rOCT1(L447Y,Q448E) versus rOCT1 (Gorboulev et al., 2005). Similarly, we observed no effects of mutations C451M,

L447Y, and/or Q448E on half maximal activation of TEA⁺-induced currents at -50mV ($I_{0.5(\text{TEA})}$). The ($I_{0.5(\text{TEA})}$) values were: rOCT1: $65 \pm 16\mu\text{M}$, rOCT1(C451M): $65 \pm 18\mu\text{M}$, rOCT1(C451M,L447Y): $82 \pm 16\mu\text{M}$, rOCT1(C451M,Q448E): $57 \pm 22\mu\text{M}$, and rOCT1(C451M,L447Y,Q448E): $98 \pm 42\mu\text{M}$ (n = 5-7 each) (for examples see Fig. 1B). The data suggest that mutations C451M, L447Y, Q448E are not critical for low-affinity binding of TEA⁺ to rOCT1 (Gorbunov et al., 2008).

Inhibition of rOCT1 and Mutants by Extracellular Corticosterone.

Previously we observed that corticosterone inhibited uptake of $10\mu\text{M}$ [¹⁴C]TEA⁺ in oocytes expressing wildtype rOCT1 or rOCT1(L447Y,Q448E) with IC₅₀ values of $198\mu\text{M}$ and $5.3\mu\text{M}$, respectively (Gorboulev et al., 2005). In these experiments we preincubated the oocytes with corticosterone and measured TEA⁺ uptake after 30min incubation with [¹⁴C]TEA⁺ in the presence of corticosterone. These experimental conditions do not allow to distinguish whether the mutations change the affinity of corticosterone to the outward- or inward-facing substrate binding cleft because corticosterone slowly permeates the plasma membrane by passive diffusion (Arndt et al., 2001; Volk et al., 2003). To measure the interaction of corticosterone with the outward-facing cleft, we superfused oocytes for 45s at -50mV with 0.2mM or 2mM TEA⁺ in the presence of various concentrations of corticosterone and determined the IC_{50(cort.)} values (Table 1). The IC_{50(cort.)} values from current measurements with 2mM TEA⁺ were 3.5-4.7 times higher than from measurements with 0.2mM TEA⁺. Since for competitive inhibition a factor of 7.59 and for non-competitive inhibition a factor of 1 is predicted, the interaction between TEA⁺ and corticosterone can be described as partially competitive. Considering the observed degrees of partial competition (see Methods) we estimated the K_i values for corticosterone $K_{i(\text{cort.})}$ from the IC_{50(cort.)} values from current measurements with 0.2mM TEA⁺ (Figs. 2, 3, 5 and Table 1).

For inhibition of wildtype rOCT1 and rOCT1(C451M) by extracellular corticosterone, respective $K_{i(\text{cort.})}$ values of $27.8 \pm 7.2\mu\text{M}$ and $18.4 \pm 1.9\mu\text{M}$ were estimated (Fig. 2, Table 1). As these values differ not significantly, the data suggest that the exchange of Cys451 by methionine does not alter the affinity of corticosterone to the outward-facing substrate binding pocket. Significantly lower $\text{IC}_{50(\text{cort.})}$ and $K_{i(\text{cort.})}$ ($3.3 \pm 0.3 \mu\text{M}$) values were obtained for corticosterone inhibition of TEA^+ currents in rOCT1(C451M,L447Y,Q448E) versus the control rOCT1(C451M) (Figs. 2, 3, Table 1). To elucidate whether the mutation L447Y or Q448E is responsible for the affinity increase, we measured the inhibition of TEA^+ -induced currents by corticosterone in the mutants rOCT1(C451M,L447Y) and rOCT1(C451M,Q448E) (Fig. 3, Table 1). For rOCT1(C451M,L447Y) a $K_{i(\text{cort.})}$ of $5.0 \pm 0.5\mu\text{M}$ was obtained (Fig. 3, Table 1). This value is significantly lower than the $K_{i(\text{cort.})}$ of rOCT1 or rOCT1(C451M) and similar to the $K_{i(\text{cort.})}$ of rOCT1(C451M,L447Y,Q448E). The data indicate that the L447Y mutation is responsible for the increase in affinity for corticosterone from the extracellular side. Consistently, the $K_{i(\text{cort.})}$ value estimated for mutant rOCT1(C451M,Q448E) ($20.0 \pm 4.2\mu\text{M}$) is not significantly different from wildtype rOCT1 or rOCT1(C451M) (Fig. 3, Table 1).

Inhibition of rOCT1 and Mutants by Intracellular Corticosterone. To measure the affinity of corticosterone to the inward-facing substrate binding cleft, oocytes expressing mutants of rOCT1 were preincubated for 10min with various concentrations of corticosterone, extracellular corticosterone was then removed by washing, and inward currents induced by superfusion with 0.2mM or 2mM TEA^+ were measured. In oocytes expressing rOCT1(C451M) or rOCT1(C451M,Q448E), the IC_{50} values for corticosterone inhibition of currents induced by 2mM TEA^+ are 2.6 or 2-times higher compared to those induced by 0.2mM TEA^+ (Fig. 4, Table 1).

This suggests some competition between intracellular corticosterone and TEA⁺ that had entered the oocytes during the measurements. At variance, in oocytes expressing rOCT1(C451M,L447Y) similar IC_{50(cort.)} values were obtained for inhibition of currents induced by 0.2mM or 2mM TEA⁺ (Fig. 4, Table 1). This indicates that TEA⁺ does not replace corticosterone from the inward-facing cleft of this mutant.

In oocytes expressing rOCT1(C451M) intracellular corticosterone inhibited inward currents by 0.2mM TEA⁺ with an IC_{50(cort.)} value of 132 ± 34μM (Fig. 4, Table 1). Considering the small degree of competition between intracellular corticosterone and TEA⁺, a K_{i(cort.)} value of 71 ± 19μM was obtained (Table 1). This value is significantly higher compared to the K_{i(cort.)} for corticosterone inhibition from extracellular side (P < 0.001) suggesting that intracellular corticosterone binds with lower affinity to rOCT1 than corticosterone present at the extracellular side. This is at variance to rOCT2 where corticosterone binds with higher affinity from the intracellular side (Volk et al., 2003).

In oocytes expressing rOCT1(C451M,L447Y), IC_{50(cort.)} values of 28 ± 4μM (0.2mM TEA⁺) and 25 ± 3μM (2mM TEA⁺) were determined and a K_{i(cort.)} value of 28 ± 4μM was estimated (Fig. 4, Table 1). Notably, this K_{i(cort.)} value is significantly lower than the K_{i(cort.)} value of rOCT1(C451M) from the intracellular side. The data indicate that replacement of Leu447 by tyrosine increases the affinity of corticosterone to both, the outward-facing and inward-facing substrate pocket.

We also measured the effect of replacement of Gln448 by glutamate on the affinity of intracellular corticosterone (Fig. 4). In oocytes expressing rOCT1(C451M,Q448E) intracellular corticosterone inhibited TEA⁺-induced inward currents with a K_{i(cort.)} of 2.7 ± 0.4μM. This is significantly lower than the K_{i(cort.)} determined for intracellular interaction of corticosterone with rOCT1(C451) (Table

1). It is also significantly lower than the $K_{i(\text{cort.})}$ value of $20.0 \pm 4.2\mu\text{M}$ estimated for the extracellular interaction of corticosterone with rOCT1(C451M,Q448E) ($P < 0.001$). The data indicate that the higher affinity of corticosterone to the inward- compared to the outward-facing substrate binding pocket of rOCT2 can be transferred to rOCT1 by exchange of Gln448 with glutamic acid located in the corresponding position of rOCT2.

First-Round-Simulations of Corticosterone Binding to the Outward- and Inward-facing Clefts of rOCT1. To distinguish whether the identified amino acids interact directly with corticosterone or exhibit indirect effects on the corticosterone binding site(s) we modelled the interaction of corticosterone with rOCT1. Previously we described a model of the inward-facing conformation of rOCT1, which was obtained from the crystal structure of *E. coli* lactose permease (LacY) that belongs to the same superfamily as rOCT1 (Popp et al., 2005). The quality of this model was demonstrated by showing that seven amino acids that are critical for substrate affinity and/or selectivity, line the solvent accessible surface of the modelled inward-open cleft. Using the alternating access transport model of LacY that has been derived on the basis of sophisticated functional and biophysical data (Kaback et al., 2007; Majumdar et al., 2007; Smirnova et al., 2006) we also modelled the outward-facing conformation of rOCT1 (Gorbunov et al., 2008). In the present study the interactions of corticosterone with the outward- and inward-facing conformation of rOCT1 were simulated by docking of corticosterone to the transporter models. 28 of 30 corticosterone molecules that docked with the highest scores to the inward-facing cleft of rOCT1, and the 30 corticosterone molecules that docked with the highest scores to the outward-facing cleft, have distances to Leu447 smaller than 10.6 \AA (center of gravity used for corticosterone, thus the shortest distance between Leu447 and corticosterone is usually between $5\text{-}6\text{ \AA}$). We used the

results with the smallest distances between corticosterone and Leu447 to select additional amino acid candidates that may be accessible for interaction with extracellular and intracellular corticosterone for mutagenesis experiments. By this procedure Phe160 in TMH2 and Tyr222 in TMH4 could be identified as good candidates.

Inhibition of rOCT1(C451M,F160A) and rOCT1(C451M,Y222F) by Corticosterone. We tested whether the replacement of Phe160 by alanine or of Tyr222 by phenylalanine would change the affinities for extracellular and/or intracellular corticosterone. First we determined whether the affinity of TEA⁺ is altered in rOCT1(C451M,F160A). For currents induced by TEA⁺ at -50mV, an $I_{0.5(\text{TEA})}$ value was obtained ($98 \pm 13\mu\text{M}$, $n = 4$) that is similar to rOCT1(C451M) and rOCT1. Extracellular corticosterone inhibited TEA⁺-induced currents by rOCT1(C451M,F160A) with a $K_{i(\text{cort.})}$ value of $6.9 \pm 1.8\mu\text{M}$ which is significantly smaller compared to rOCT1(C451M) or rOCT1 (Fig. 5, Table 1). Importantly, a significantly smaller $K_{i(\text{cort.})}$ value for rOCT1(C451M,F160A) compared to rOCT1(C451M) was also determined when corticosterone was applied from the intracellular side ($18 \pm 4\mu\text{M}$ versus $71 \pm 19\mu\text{M}$) (Fig. 5, Table 1).

Previous data showed that exchange of Tyr222 by phenylalanine decreased the K_m value for [¹⁴C]TEA⁺ uptake (Popp et al., 2005). Conformingly, the $I_{0.5(\text{TEA})}$ value for currents induced by TEA⁺ (-50mV) was decreased in rOCT1(C451M,Y222F) compared to rOCT1(C451M) ($39 \pm 2\mu\text{M}$ versus $65 \pm 18\mu\text{M}$, $n = 5$ each, $P < 0.05$). In oocytes expressing rOCT1(C451M,Y222F), $K_{i(\text{cort.})}$ values of $26.2 \pm 1.7\mu\text{M}$ and $69 \pm 15\mu\text{M}$ were determined for inhibition of TEA⁺-induced currents by extracellular and intracellular corticosterone, respectively (Table 1). The values are similar to the $K_{i(\text{cort.})}$ values measured in oocytes expressing rOCT1(C451M) or rOCT1 (Table 1). The data suggest that Phe160 clearly participates in binding of

extracellular and intracellular corticosterone to rOCT1 and that Tyr222 is not critically involved in corticosterone binding.

Second-Round-Simulations of Corticosterone Binding. Since the above described mutagenesis experiments revealed that the affinities of corticosterone to both, the outward-facing and inward-facing conformation of rOCT1 were increased when Leu447 in TMH10 was replaced by tyrosine or when Phe160 in TMH2 was replaced by alanine, we performed a new set of docking simulations in which residues Leu447 and Phe160 were selected as direct docking sites using radii of 5Å around these residues. The obtained 30 docking sites for corticosterone with the highest interaction energies for the outward- and inward-facing conformation of rOCT1 clustered into families of conformers with similar distances between corticosterone and the target amino acids but slightly different orientations of corticosterone in the putative binding pocket. Fig. 6 shows one example for the interaction of corticosterone with the inward facing cleft. Note, that the model is consistent with the interaction of corticosterone with Phe160 (distance 2.6Å) and Leu447 (distance 4.9Å). It also suggests an interaction with Trp218 in TMH4 (distance 4.0Å), Arg440 in TMH10 (distance 2.8Å), and Asp475 in TMH11 (distance 2.8 Å). The docking model does not support a direct interaction of corticosterone with Tyr222 (distance 8.5Å) and Gln448 (distance 7.6Å). We speculate that the affinity increase for intracellular corticosterone observed after exchange of Gln448 by glutamate might be due to an allosteric effect on Leu447.

In Fig. 7 an example for the interaction of corticosterone with the outward-facing substrate binding cleft is shown. The figures show that corticosterone is located close to Phe160 (3.6Å), Leu447 (5.0Å), Trp218 (3.0Å), Arg440 (3.1Å) and Asp475 (2.8Å). The distances of corticosterone to Tyr222 (6.0Å) and Gln448 (6.4Å) are larger and do not yield a direct van der Waals contact. This is consistent with the

missing effects of these mutations on inhibition of rOCT1 by extracellular corticosterone.

Affinity of Corticosterone to rOCT1(C451M,W218Y) and rOCT1(C451M,R440K). The modelled interactions of corticosterone with rOCT1 predict that mutations of Trp218, Arg440 and Asp475 can change the inhibition of TEA⁺-induced currents by intracellular and extracellular corticosterone. For TEA⁺-induced currents by rOCT1(C451M,W218Y) and by rOCT1(C451M,R440K) measured at -50mV, $K_{0.5(\text{TEA})}$ values of $67 \pm 4\mu\text{M}$ and $67 \pm 6\mu\text{M}$ ($n = 3$, each) were determined. Since these values are similar to rOCT1 and rOCT1(C451M) the two amino acids are not critical for the affinity of TEA⁺ to stimulate inward currents. In Fig. 8 we measured TEA⁺-induced currents by rOCT1(C451M,W218Y) in the presence of extracellular or intracellular corticosterone. With 1mM corticosterone applied to the extracellular or intracellular side, a significantly lower inhibition was observed compared to rOCT1(C451M) or wildtype rOCT1 ($P < 0.01$ for difference). This suggests a reduced maximal inhibition and is consistent with an interaction of extracellular and intracellular corticosterone with Trp218. Using the variant rOCT1(C451M,W218Y) we also observed an atypical stimulation at low concentrations of extracellular or intracellular corticosterone on currents that were induced by 2mM TEA⁺. This stimulation may be explained by binding of corticosterone to a high-affinity binding site (Volk et al., 2003) which may be located in a peripheral part of the binding cleft and may stimulate TEA induced current in this specific mutant. The low degree of maximal inhibition and the atypical curves obtained with 2mM TEA⁺ prevents a determination of $\text{IC}_{50(\text{cort.})}$ values for most experimental conditions. For partial inhibition of TEA⁺ (0.2mM) induced currents by extracellular corticosterone we determined an $\text{IC}_{50(\text{cort.})}$ value of $333 \pm 42\mu\text{M}$ ($n = 4$). Assuming competitive inhibition we estimated a minimal

$K_{i(\text{cort.})}$ value ($93.3 \pm 11.8\mu\text{M}$), which is significantly higher than the $K_{i(\text{cort.})}$ values obtained for rOCT1 or rOCT1(C451M) (Table 1).

Fig. 9 shows corticosterone inhibition of TEA^+ -induced currents in oocytes expressing rOCT1(C451M,R440K). For inhibition of TEA^+ -induced currents with extracellular corticosterone IC_{50} values of $112 \pm 15\mu\text{M}$ (0.2mM TEA^+) and $588 \pm 124\mu\text{M}$ (2mM TEA^+) were determined suggesting partial competitive inhibition (Table 1). The estimated K_1 value of $40.4 \pm 5.3\mu\text{M}$ is significantly higher compared to rOCT1 wildtype or rOCT1(C451M). The maximal inhibition of rOCT1(C451M,R440K) by intracellular corticosterone is significantly smaller compared to rOCT1(C451M) or wildtype rOCT1. Upon preincubation of oocytes expressing rOCT1(C451M,R440K) with 1mM corticosterone currents induced by 0.2mM TEA^+ were inhibited by $44 \pm 4\%$ versus $93 \pm 5\%$ in oocytes expressing rOCT1(C451M) ($P < 0.01$ for difference). For inhibition by intracellular corticosterone of currents induced by 0.2mM TEA an IC_{50} value of $124 \pm 33\mu\text{M}$ could be obtained (Table 1). This value is similar to the IC_{50} value of wildtype rOCT1 suggesting an unaltered affinity for corticosterone. The data showing reduced affinity of extracellular corticosterone and reduced maximal inhibition by intracellular corticosterone are consistent with an interaction of corticosterone with Arg440 in the outward- and inward-facing conformation.

Since mutations of Asp475 block or drastically reduce organic cation transport by rOCT1 in oocytes (Gorboulev et al., 1999), effects of mutations in this position on the inhibition of TEA^+ induced currents by extracellular versus intracellular corticosterone could not be investigated. However, in HEK293 cells stably transfected with rOCT1(D475E) the inhibition of [^3H]MPP uptake by extracellular or intracellular corticosterone could be measured. Uptake measurements were performed using a 1s incubation period with $0.013\mu\text{M}$ [^3H]MPP $^+$. Inhibition by

extracellular corticosterone was measured by performing the 1s incubation with [^3H]MPP $^+$ in the presence of corticosterone. To measure inhibition by intracellular corticosterone, the cells were pre-incubated for 10 min with corticosterone. Thereafter the cells were diluted with 15-fold excess of corticosterone-free buffer containing 0.013 μM [^3H]MPP $^+$, and uptake of MPP $^+$ was measured after 1s incubation. For inhibition of wildtype rOCT1 and rOCT1(D475E) mutant by extracellular corticosterone, $K_{i(\text{cort})}$ values of $6.9 \pm 0.9 \mu\text{M}$ and $72.5 \pm 11.8 \mu\text{M}$ were determined, respectively ($P < 0.001$ for difference, $n = 3$ each). The $K_{i(\text{cort})}$ values for inhibition by intracellular corticosterone were $8.5 \pm 1.0 \mu\text{M}$ for rOCT1 versus $357 \pm 55 \mu\text{M}$ for rOCT1(D475E) ($P < 0.01$ for difference, $n = 3$ each)².

Effects of Mutations Changing the Interaction of Corticosterone on the Affinity of MPP $^+$. We determined the $\text{IC}_{50(\text{MPP})}$ values for inhibition of [^{14}C]TEA $^+$ (5 μM) uptake by MPP $^+$ (Table 2). Because 5 μM [^{14}C]TEA $^+$ used for uptake was more than 10-fold smaller than the K_m values for TEA $^+$ in wildtype rOCT1 and the tested mutants, the obtained $\text{IC}_{50(\text{MPP})}$ values are basically identical to the $K_{i(\text{MPP})}$ values. Confirming previous data (Arndt et al., 2001; Gorboulev et al., 2005), we obtained similar $\text{IC}_{50(\text{MPP})}$ values for rOCT1 ($7.4 \pm 1.1 \mu\text{M}$) and rOCT1(C451M) ($9.4 \pm 1.3 \mu\text{M}$). Previously we observed that in the mutant rOCT1(L447Y,Q448E) the K_i value for inhibition of [^{14}C]TEA $^+$ uptake by MPP $^+$ ($K_{i(\text{MPP})}$) was decreased 10-fold compared to rOCT1 (Gorboulev et al., 2005). The $\text{IC}_{50(\text{MPP})}$ value of rOCT1(C451M,L447Y,Q448E) was about 20-fold lower ($0.31 \pm 0.05 \mu\text{M}$). A similar low $\text{IC}_{50(\text{MPP})}$ value was obtained for rOCT1(C451M,L447Y) ($0.46 \pm 0.09 \mu\text{M}$). Interestingly, also the $\text{IC}_{50(\text{MPP})}$ value of rOCT1(C451M,Q448E) ($2.4 \pm 0.52 \mu\text{M}$) was significantly smaller compared to rOCT1 or rOCT1(C451M). Apparently both mutations, L447Y and Q448E, increase the affinity of MPP $^+$, however, their effects are not additive.

For mutants F160A, W218Y and R440K a decreased affinity of MPP^+ to inhibit $^{14}\text{C}]\text{TEA}^+$ uptake was observed (Table 2). $\text{IC}_{50(\text{MPP})}$ values of $19.5 \pm 2.0\mu\text{M}$ (rOCT1(C451M,F160A)), $23.1 \pm 2.2\mu\text{M}$ (rOCT1(C451M,W218Y)) and $18.6 \pm 2.2\mu\text{M}$ (rOCT1(C451M,R440K)) were determined. Previous data showed that the affinity of MPP^+ was not changed when Asp475 was replaced by glutamate (Goeboulev et al., 1999). The data suggest that Phe160, Trp218, Arg440, Leu447 and Gln448 are located within or close to the transport relevant binding site for MPP^+ and that this MPP^+ binding site is located within the innermost cavity of the binding cleft where corticosterone also binds.

Effects of Mutations Changing the Interaction of Corticosterone on the Affinity of TBuA^+ . We investigated whether mutations L447Y, F160A, W218Y and R440K altered the inhibition of TEA^+ -induced currents (-50mV) by the nontransported rOCT1 inhibitor TBuA^+ (Table 3, Fig. 10). In the mutants rOCT1(C451M,F160A) and rOCT1(C451M,L447Y) the affinity for TBuA^+ was increased at least 10-fold compared to rOCT1(C451M) whereas it was unaltered in rOCT1(C451M,W218Y) and rOCT1(C451M,R440K). The increase of the $\text{IC}_{50(\text{TBuA})}$ values for inhibition of currents induced by 2mM TEA^+ versus 0.2mM TEA^+ suggest competitive inhibition for the mutants rOCT1(C451M), rOCT1(C451M,L44Y), rOCT1(C451M,W218Y) and rOCT1(C451M,R440K). In case of rOCT1(C451M,F160A) we observed a significantly higher difference of $\text{IC}_{50(\text{TBuA})}$ values obtained with 2mM TEA^+ versus 0.2mM TEA^+ (15.8-fold) as expected for competitive inhibition (7.6-fold). This suggests allosteric effects of TEA^+ binding on TBuA^+ binding. Previous data showed that the affinity of TBuA^+ to inhibit uptake of TEA^+ was increased when Asp475 was replaced by glutamate. The data suggest that Phe160, Leu447 and Asp475 are involved in binding of extracellular TBuA^+ in addition to extracellular corticosterone.

Simulation of TBuA⁺ Binding to the Outward-facing Cleft of rOCT1. We also simulated the binding of TBuA⁺ to the outward-facing cleft of our rOCT1 homology model. Several putative interaction sites showed up if all residues lining the interior of the outward-facing cleft were allowed for docking. This may reflect the presence of low and high affinity binding sites for TBuA⁺ that were demonstrated by measuring TBuA⁺ effects on the fluorescence of rOCT1 labelled with a fluorescent dye (Gorbunov et al., 2008). Since previous data suggested that TBuA⁺ binds to Asp475 and that Asp475 is located within a transport relevant binding site for TEA⁺ (Gorboulev et al., 1999) we performed a simulation in which the allowed distance between TBuA⁺ and Asp475 was restricted to 6.5Å (Fig.11). Simulation of TBuA⁺ binding under this constraint suggested that TBuA⁺ binds simultaneously to Asp475 (3.5Å), Trp218 (4.3Å) and Phe160 (3.9Å) but does not interact with Leu447 (7.2Å), Tyr222 (7.6Å) and Arg440 (10.9Å). The observation that the affinity of TBuA was not changed in the W218Y mutant may be due to a similar hydrophobic interaction of TBuA⁺ with the indole ring of Trp218 and the phenyl ring of Phe218 (see lower panel of Fig. 11). The distance of 7.2Å between TBuA⁺ and Leu447 suggests no interaction in rOCT1 wildtype. However, after replacement of Leu447 by tyrosine the distance to the docked TbuA⁺ is shortened by about 3Å. This would allow direct contact of TBuA⁺ with tyrosine in position 447 and may explain why the affinity of TBuA⁺ was increased in the L447Y mutant (Table 3).

Discussion

We have identified five amino acid residues located within the central part of the transport path of rOCT1 that are critical for the inhibition of rOCT1 by extracellular

and intracellular available corticosterone. These amino acids contribute to the modelled outward- and inward-facing binding sites for corticosterone and are located within innermost cavities of the binding clefts. Our data suggest that three of these amino acids are also critical for binding of the non-transported inhibitor TBuA^+ from the extracellular side. Four of the amino acids within the innermost cavities are likely to be also involved in binding of the substrate MPP^+ whereas one amino acid probably interacts with TEA^+ .

Analysis of Corticosterone Interaction with rOCT1. To determine the interaction of corticosterone from both sides of the plasma membrane, electrical measurements in voltage clamped oocytes expressing rOCT1 mutants were employed. Voltage clamped conditions were used since corticosterone binding to rOCT2 was shown to be influenced by the membrane potential (Volk et al., 2003). We performed the present study with rOCT1 because several amino acids within the substrate binding region have been identified in this subtype (Gorboulev et al., 1999; Gorboulev et al., 2005; Gorbunov et al., 2008; Popp et al., 2005). The technical problem that substrate-induced currents by rOCT1 are 5-10fold lower than those by rOCT2 was solved by introducing the mutation C451M, which increases rOCT1-mediated currents without altering the interaction with corticosterone. To investigate the interaction of extracellular corticosterone with rOCT1, oocytes were superfused for 45s with TEA^+ in the presence of corticosterone. During this time period passive permeation of corticosterone across the plasma membrane can be neglected since the inhibitory effect of corticosterone could be reversed by a short wash. To investigate the interaction of corticosterone from the intracellular side we preincubated the oocytes for 10min with corticosterone, removed the extracellular corticosterone by washing, and measured currents that were induced by a short superfusion with TEA^+ . The intracellular concentration of corticosterone was

estimated by assuming that corticosterone had fully equilibrated within the intracellular aqueous phase. The validity of this assumption was verified by control experiments with rOCT1 (see Methods) and in previous experiments with rOCT2 in which preincubation with intact oocytes was compared with measurements using inside-out giant patches (Volk et al., 2003).

Since corticosterone was supposed to interact with the substrate binding region of rOCT1 that includes a binding site for TEA⁺, we measured TEA⁺- induced currents at two different TEA⁺ concentrations. This allowed us to determine the degree of competition between corticosterone and TEA⁺ and to estimate the apparent K_i value for corticosterone. Effects of mutations on the K_i value for inhibition of TEA⁺ induced currents are supposed to reflect changes at the binding site for corticosterone. The degree of competition between TEA⁺ and corticosterone may be changed when the corticosterone binding site, the TEA⁺ binding site, and/or an overlapping part of both binding sites is altered. Another possibility is that a short term allosteric interaction between the two sites is affected. In wildtype rOCT1 and the rOCT1(C451M) mutant we observed competition between TEA⁺ and extracellular as well as intracellular corticosterone. This competition was affected by some of the applied mutations. At the outward-facing corticosterone binding site the degree of competition between corticosterone and TEA⁺ was unaltered when Leu447 was replaced by tyrosine but was decreased when Phe160 was exchanged for alanine. At variance intracellular competition between corticosterone and TEA⁺ was abolished when Leu447 was replaced by tyrosine whereas it was not changed in the F160A mutant (Table 1, compare $f_{(\text{part.compet.})}$ values). These effects suggest different orientations and/or positions of Phe160 and Leu447 in the outward-facing versus the inward-facing conformation.

TEA⁺ probably does not bind directly to the four amino acids that interact with corticosterone (Phe160, Trp218, Arg440, Leu447) because the $I_{(0.5)}$ values for TEA⁺-induced currents were not altered by mutations in these positions. However, the TEA⁺ binding site supposedly overlaps with the binding site of corticosterone since Asp475, which is critical for the affinity of TEA⁺ (Gorboulev et al., 1999), is located within the modelled innermost cavities and mutation of this site alters the affinity of extracellular and intracellular corticosterone.

Model Analysis of Corticosterone and TBuA⁺ Binding. Modelling of the inward-open and outward-open conformations of rOCT1 on the basis of LacY permease has been discussed in detail earlier (Popp et al. 2005, Gorbunov et al. 2008). The sequence identity between rOCT1 and LacY is low (~ 12 %), however, different sequence alignment programs produced consistent alignments. LacY-based models of rOCT1 exhibited no steric clashes after refinement indicating a similar packing in OCT1 and LacY. The quality of the modelled inward-facing conformation is exemplified by the observation that seven amino acids that are critical for affinities of substrates line the inward open cleft (Popp et al. 2005).

The model of the outward-facing conformation of rOCT1 was constructed in analogy to an experimentally verified model of LacY assuming a rigid-body movement of TMHs 1-6 with respect to TMHs 7-12 allowing intrahelix motions and drifting of individual domains (Gorbunov et al. 2008). An experimental indication for the quality of this model was the observation that amino acids in TMH2 and TMH11 that have contact in the modelled inward-facing conformation and are far apart in the modelled outward-facing conformation proved to be critical for transporter function after high affinity binding of TBuA⁺ (Gorbunov et al. 2008).

Being aware of the limitations in modelling ligand-transporter interactions using modelled tertiary structures, our first attempt only aimed to evaluate whether the

experimental observation that Leu447 interacts with extracellular and intracellular corticosterone is consistent with the structural models. This turned out to be the case, however, the exact position of corticosterone close to Leu447 was not defined. After Phe160 was identified by mutagenesis as another amino acid that interacts with extracellular and intracellular corticosterone, we performed a second round of docking analyses restricting the distances between corticosterone and the rOCT1 residues Leu447 and Phe160 for distinguishing successful and unsuccessful docking. Using this approach Trp218, Arg440 and Asp475 were predicted as additional amino acids interacting with extracellular and intracellular corticosterone. The functional analyses of mutations in these positions are consistent with these predictions. They revealed that the affinity of extracellular corticosterone was decreased after mutation of Trp218, the maximal inhibition by extracellular corticosterone was decreased after mutation of Arg440, and the maximal inhibition by intracellular corticosterone was decreased after mutation of both positions. Note, that a mutation of an amino acid interacting with corticosterone must not necessarily change the dissociation constant for corticosterone. It may alter the positioning of bound corticosterone without changing its dissociation constant. This might then lead to an altered degree of maximal inhibition. The modelled position of Asp475 in the outward-facing and inward-facing binding site of corticosterone was confirmed experimentally by showing that the affinity of extracellular and intracellular corticosterone was decreased when Asp475 was replaced by glutamate. Since most mutations in position 475 block transport activity and the most conservative replacement (Asp475Glu) decreases transport activity drastically, a different expression system and a different transport assay had to be employed to determine the affinity of extracellular and intracellular corticosterone to this mutant (H. Koepsell, V. Gorboulev, U. Roth, unpublished data).

The structural models of rOCT1 are also consistent with our observations that the affinity for extracellular corticosterone was unchanged after mutation of Gln448 and that the affinity for corticosterone from both sides was unaltered when Tyr222 was mutated. On first sight the affinity increase of intracellular corticosterone after mutation of Gln448 appears to contradict our corticosterone-interaction modelling. However, the replacement of Gln448 by glutamate may change the position of Leu447, which directly interacts with corticosterone.

The quality of the modelled outward-facing cleft of rOCT1 was also supported by simulation of TBuA⁺ binding to the outward-facing cleft and mutagenesis. The simulation revealed several putative TBuA⁺ interaction sites within the cleft that may represent high and low affinity TBuA⁺ binding sites. Recently we identified high and low affinity interaction of TBuA⁺ with rOCT1 using voltage-clamp fluorometry (Gorbunov et al., 2008). Mutagenesis at all simulated interaction sites combined with TBuA⁺ binding measurements is required to identify binding sites with different affinities. Since we hypothesized that the transport relevant TBuA⁺ binding site is located within the innermost part of the cleft, and previous mutagenesis suggested interaction of Asp475 with TBuA⁺, we performed a simulation in which the distance of TBuA⁺ to Asp475 was restricted. This simulation suggests that TBuA⁺ binds to Phe160 and Trp218 in addition to Asp475. Interaction of TBuA⁺ with Phe160 is supported by the observed increase of TBuA⁺ affinity after replacement of Phe160 with alanine (Table 3). So far, the simulated interaction of TBuA⁺ with Trp218 has not been verified since the affinity of TBuA⁺ remained unchanged when Trp218 was replaced by phenylalanine. This does not contradict our simulation, which predicts a hydrophobic interaction of a butyl side chain of TBuA⁺ with the aromatic ringsystem of Trp218 because this interaction may be mimicked by the aromatic ring of phenylalanine (see lower panel of Fig. 11).

Future experiments will show whether the affinity of TBuA⁺ is changed when amino acids with aliphatic side chains are used for substitution of Trp218. Our simulation showing a distance of 6.2Å between Leu447 and TBuA does not support a direct interaction of TBuA⁺ with Leu447 in wildtype rOCT1. However, in the L447Y mutant the distance between TBuA⁺ and Tyr447 should be around 3Å allowing a direct interaction of TBuA⁺ which may lead to the observed increase in affinity.

Subtype and Species Differences of Corticosterone Binding. Employing preincubation of oocytes with corticosterone, the rank order of the apparent K_i values for corticosterone inhibition of organic cation uptake is hOCT3 \ll rOCT3 = rOCT2 \ll rOCT1 (Gorboulev et al., 2005, Koepsell et al., 2007). Four of the five amino acids that are supposed to be directly involved in corticosterone binding to rOCT1 (Phe160, Trp218, Arg440 and Asp475, numbering of rOCT1) are conserved between rOCT1, rOCT2, rOCT3 and hOCT3 whereas the amino acids in positions 447 differ between rOCT1 versus rOCT2, rOCT3 or hOCT3 (Fig. 12). Since the affinity of corticosterone is similar when tyrosine (rOCT2) or phenylalanine (rOCT3, hOCT3) is placed into position 447 of rOCT1 (C. Volk, V. Gorboulev, H. Koepsell, unpublished data) and rOCT3 and hOCT3 have identical amino acids in all five positions but different affinities to corticosterone, the higher affinities of corticosterone to rOCT2, rOCT3 and hOCT3 versus rOCT1 cannot be exclusively due to differences in position 447. Considering the differences in substrate selectivity between OCT subtypes and OCT3 orthologs, and the overlap between the substrate and corticosterone binding sites we speculate that the corticosterone binding sites of OCT subtypes and orthologs contain more structural differences than implicated from our studies that have been mostly performed within the rOCT1 backbone. It is possible that not all amino acids that interact with corticosterone in

rOCT1 also participate in corticosterone binding to the other subtypes and orthologs.

Mechanism for Transport by rOCT1. Our data indicating outward-facing and inward-facing innermost cavities in rOCT1 that contain several identical amino acids which are critical for affinities of nontransported inhibitors (corticosterone, TBuA⁺) and substrates (MPP⁺, TEA⁺) strongly suggest that rOCT1 operates by an alternating access transport mechanism. In a *trans*-zero transport cycle, an organic cation binds to the outward-facing innermost cavity, the cavity closes on the extracellular and opens on the intracellular side, the cation is released to the cytosol, and the empty cavity switches back to the outward-facing conformation. Non-transported inhibitors like the bulky rectangular corticosterone molecule with the dimensions of $14 \times 7 \times 5 \text{ \AA}$ may bind to the innermost cavities and may thereby block the conformational switch. Recently we provided evidence for the existence of high affinity organic cation binding sites in OCTs and demonstrated that high affinity binding of organic cations may lead to inhibition of transport (Gorbunov et al., 2008; Minuesa et al. 2009). We speculate that these high affinity binding sites are located outside the innermost cavities in more peripheral regions of the binding clefts and are not directly involved in translocation.

Recent experimental data also suggest the existence of outward-open and inward-open innermost cavities in rOCT2 and provide support for an alternating access transport mechanism by this subtype (Schmitt et al., 2009). We observed that small cations are taken up at 0mV together with organic cation substrates and provided evidence that this effect cannot be explained by opening of passive permeabilities during transport. Interestingly, the surplus of charge translocation was abolished when Glu448 in the innermost cavity of rOCT2 corresponding to Gln448 in rOCT1 was replaced by glutamine. We speculate that Glu448 and

Asp475 within the outward-facing innermost cavity of rOCT2 attract small cations and release them from the inward-facing innermost cavity in which Glu448 is located more peripherally compared to the outward-facing innermost cavity (see Figs. 6 and 7).

Acknowledgements: We thank Michael Christof for preparing the figures.

References

- Abramson J, Smirnova I, Kasho V, Verner G, Kaback HR and Iwata S (2003)
Structure and mechanism of the lactose permease of *Escherichia coli*. *Science (Wash DC)* **301**:610 -615.
- Arndt P, Volk C, Gorboulev V, Budiman T, Popp C, Ulzheimer-Teuber I, Akhoundova A, Koppatz S, Bamberg E, Nagel G and Koepsell H (2001)
Interaction of cations, anions, and weak base quinine with rat renal cation transporter rOCT2 compared with rOCT1. *Am J Physiol Renal Physiol* **281**:F454-F468.
- Budiman T, Bamberg E, Koepsell H and Nagel G (2000) Mechanism of electrogenic cation transport by the cloned organic cation transporter 2 from rat. *J Biol Chem* **275**:29413-29420.
- Ermolova N, Madhvani RV and Kaback HR (2006) Site-directed alkylation of cysteine replacements in the lactose permease of *Escherichia coli*: helices I, III, VI, and XI. *Biochemistry* **45**:4182-4189.
- Gorboulev V, Shatskaya N, Volk C and Koepsell H (2005) Subtype-specific affinity for corticosterone of rat organic cation transporters rOCT1 and rOCT2 depends on three amino acids within the substrate binding region. *Mol Pharmacol* **67**:1612-1619.
- Gorboulev V, Volk C, Arndt P, Akhoundova A and Koepsell H (1999) Selectivity of the polyspecific cation transporter rOCT1 is changed by mutation of aspartate 475 to glutamate. *Mol Pharmacol* **56**:1254-1261.

- Gorbunov D, Gorboulev V, Shatskaya N, Mueller T, Bamberg E, Friedrich T and Koepsell H (2008) High-affinity cation binding to organic cation transporter 1 induces movement of helix 11 and blocks transport after mutations in a modelled interaction domain between two helices. *Mol Pharmacol* **73**:50-61.
- Ho SN, Hunt HD, Horton RM, Pullen JK and Pease LR (1989) Site-directed mutagenesis by overlap extension using the polymerase chain reaction. *Gene* **77**:51-59.
- Holyoake J and Sansom MSP (2007) Conformational change in an MFS protein: MD simulations of LacY. *Structure* **15**:873-884.
- Kaback HR, Dunten R, Frillingos S, Venkatesan P, Kwaw I, Zhang W and Ermolova N (2007) Site-directed alkylation and the alternating access model for LacY. *Proc Natl Acad Sci U S A* **104**:491-494.
- Koepsell H, Lips K and Volk C (2007) Polyspecific Organic Cation Transporters: Structure, Function, Physiological Roles, and Biopharmaceutical Implications. *Pharm Res* **24**:1227-1251.
- Lips KS, Volk C, Schmitt BM, Pfeil U, Arndt P, Miska D, Ermert L, Kummer W and Koepsell H (2005) Polyspecific cation transporters mediate luminal release of acetylcholine from bronchial epithelium. *Am J Respir Cell Mol Biol* **33**:79-88.
- Majumdar DS, Smirnova I, Kasho V, Nir E, Kong X, Weiss S and Kaback HR (2007) Single-molecule FRET reveals sugar-induced conformational dynamics in LacY. *Proc Natl Acad Sci U S A* **104**:12640-12645.
- Mehrens T, Lelleck S, Çetinkaya I, Knollmann M, Hohage H, Gorboulev V, Bokník P, Koepsell H and Schlatter E (2000) The affinity of the organic cation

transporter rOCT1 is increased by protein kinase C-dependent phosphorylation.

J Am Soc Nephrol **11**:1216-1224.

Minuesa G, Volk C, Molina-Arcas M, Gorboulev V, Erkizia I, Arndt P, Clotet B, Pastor-Anglada M, Koepsell H and Martinez-Picado J (2009) Transport of lamuvidine (3TC) and high-affinity interaction of nucleoside reverse transcriptase inhibitors with human organic cation transporters 1, 2, and 3. *J Exp Pharm Ther* **329**:252-261.

Nagel G, Volk C, Friedrich T, Ulzheimer JC, Bamberg E and Koepsell H (1997) A reevaluation of substrate specificity of the rat cation transporter rOCT1. *J Biol Chem* **272**:31953-31956.

Popp C, Gorboulev V, Müller TD, Gorbunov D, Shatskaya N and Koepsell H (2005) Amino acids critical for substrate affinity of rat organic cation transporter 1 line the substrate binding region in a model derived from the tertiary structure of lactose permease. *Mol Pharmacol* **67**:1600-1611.

Rarey M, Kramer B and Lengauer T (1999) The particle concept: placing discrete water molecules during protein-ligand docking predictions. *Proteins* **34**:17-28.

Rarey M, Kramer B, Lengauer T and Klebe G (1996) A fast flexible docking method using an incremental construction algorithm. *J Mol Biol* **261**:470-489.

Reitman ML and Schadt EE (2007) Pharmacogenetics of metformin response: a step in the path toward personalized medicine. *J Clin Invest* **117**:1226-1229.

Schmitt BM, Gorbunov D, Schlachtbauer P, Egenberger B, Gorboulev V, Wischmeyer E, Müller T, Koepsell H (2009) Charge-to-substrate ratio during

organic cation uptake by rat OCT2 is voltage dependent and altered by exchange of glutamate 448 by glutamine. *Am J Physiol Renal Physiol* **296**:F709-F722.

Smirnova I, Kasho V, Choe J-Y, Altenbach C, Hubbell WL and Kaback HR (2007)

Sugar binding induces an outward facing conformation of LacY. *Proc Natl Acad Sci U S A* **104**:16504-16509.

Smirnova IN, Kasho VN and Kaback HR (2006) Direct sugar binding to LacY

measured by resonance energy transfer. *Biochemistry* **45**:15279-15287.

Sturm A, Gorboulev V, Gorbunov D, Keller T, Volk C, Schmitt BM, Schlachtbauer

P, Ciarimboli G and Koepsell H (2007) Identification of cysteines in rat organic cation transporters rOCT1 (C322, C451) and rOCT2 (C451) critical for transport activity and substrate affinity. *Am J Physiol Renal Physiol* **293**:F767-F779.

Volk C, Gorboulev V, Budiman T, Nagel G and Koepsell H (2003) Different

affinities of inhibitors to the outwardly and inwardly directed substrate binding site of organic cation transporter 2. *Mol Pharmacol* **64**:1037-1047.

Zhang X, Shirahatti NV, Mahadevan D and Wright SH (2005) A conserved

glutamate residue in transmembrane helix 10 influences substrate specificity of rabbit OCT2 (SLC22A2). *J Biol Chem* **280**:34813-34822.

Footnotes

¹This work was supported by the Deutsche Forschungsgemeinschaft Grant SFB 487/A4.

²Note, that the $K_{i(\text{cort.})}$ value for inhibition of wildtype rOCT1 by extracellular corticosterone measured in HEK293 cells was lower compared to the $K_{i(\text{cort.})}$ value measured in *Xenopus laevis* oocytes (Table 1). Recent data suggest that these differences as well as different affinities of some organic cations observed after expression of rOCT1 in HEK293 cells versus oocytes, are due to different regulatory states of rOCT1 in the two expression systems (H. Koepsell, V. Gorboulev and U. Roth, unpublished data).

Legends for Figures

Fig. 1. Comparison of TEA⁺-induced currents in rOCT1 wildtype and mutants. Noninjected oocytes or cRNA injected oocytes were incubated for 3-5 days, clamped to -50mV, superfused with TEA⁺, and currents induced by various concentrations of TEA⁺ were measured. A) Maximal currents induced by TEA⁺ ($I_{\max(\text{TEA})}$). $I_{\max(\text{TEA})}$ values were measured by superfusion of oocytes with 2mM TEA⁺. Mean values \pm S.E.M are shown and numbers of analyzed oocytes are indicated in parentheses **P<0.01, ***P<0.001. B) Examples for measured concentration activation curves. The Michaelis Menten equation has been fitted to the data.

Fig. 2. Inhibition of TEA⁺-induced currents mediated by wildtype rOCT1 and mutant rOCT1(C451M) by extracellular corticosterone. Oocytes expressing rOCT1 wildtype or rOCT1(C451M) were clamped to -50mV and superfused with 45s long pulses of Ori buffer containing 0.2mM TEA⁺ plus various concentrations of corticosterone or 2mM TEA⁺ plus corticosterone. Each pulse with TEA⁺ was followed by short wash with Ori buffer. Currents (I) were normalized to currents measured in the absence of corticosterone (I_0) and mean values \pm S.E.M are shown. The numbers of analyzed oocytes are indicated in parentheses. The Hill equation was fitted to compiled data sets. The data show that the affinity of extracellular corticosterone to rOCT1 was not changed significantly after exchange of Cys451 by methionine.

Fig. 3. Effects of mutations in positions 447 and/or 448 of rOCT1 on inhibition of TEA⁺-induced currents by extracellular corticosterone. Mutants rOCT1(C451M,

L447Y), rOCT1(C451M,Q448E), and rOCT1(C451M,L447Y,Q448E) were expressed in oocytes, and inhibition of TEA⁺-induced currents by extracellular corticosterone was measured. The measurements were performed and the data are presented as in Fig.2. For comparison, inhibition curves obtained under identical experimental conditions in oocytes expressing rOCT1(C451M) are indicated as lines. The experiments indicate that the affinity of extracellular corticosterone was increased after replacement of Leu447 by tyrosine.

Fig. 4: Effects of mutations in positions 447 or 448 of rOCT1 on inhibition of TEA⁺-induced currents by intracellular corticosterone. Mutants rOCT1(C451M), rOCT1(C451M,L447Y) or rOCT1(C451M,Q448E) were expressed in oocytes. Oocytes were clamped to -50mV and incubated for 10min with Ori buffer containing corticosterone. Oocytes were washed with Ori buffer, and currents induced by superfusion with Ori buffer containing 0.2mM TEA⁺ or 2mM TEA⁺ were measured. The data are presented as in Fig.2. They show that the affinity of intracellular corticosterone was increased after replacement of Leu447 by tyrosine and of Gln448 by glutamic acid.

Fig. 5. Effects of the replacement of Phe160 in rOCT1(C451M) by alanine on inhibition of TEA⁺-induced currents by extracellular and intracellular corticosterone. Mutant rOCT1(C451M,F160A) was expressed in oocytes. Oocytes were clamped to -50mV and inhibition of TEA⁺-induced currents by extracellular or intracellular corticosterone was measured as in Figs. 2 and 4. For comparison, inhibition curves obtained under identical experimental conditions in oocytes expressing rOCT1(C451M) are indicated as lines. Data are presented as Figs. 2 and 4. They

show that the affinity of extracellular and intracellular corticosterone to rOCT1 was increased upon replacing Phe160 by alanine.

Fig. 6. Docking of corticosterone to the inward-facing substrate cleft of rOCT1. Stereopictures are presented showing a side view with cytosolic N- and C-termini (upper panel) and views into the binding cleft from the cytosol (middle and lower panel). The α -helices in the upper and middle panels are shown as ribbon except for TMH5 (light green) and TMH7 (green), which are presented as C α -trace in the side view for clarity. The colour code of the predicted α -helices is indicated. The lower panel shows a magnification in which the van der Waals surface of the binding cleft is coloured according to amino acid polarity, with hydrophobic residues marked in grey, polar uncharged residues in green, negatively charged residues coloured in red and positively charged amino acids in blue. The amino acid side chains of Phe160, Trp218, Tyr222, Arg440, Leu447, Gln448, and Asp475 are shown as sticks. Their positions are indicated by numbers. Putative hydrogen bonds between corticosterone (highest docking energy) and amino acids of rOCT1 are indicated by stippled lines.

Fig. 7. Docking of corticosterone to the outward-facing substrate cleft of rOCT1. A side view (upper panel) and views from the extracellular side (middle and lower panel) are shown. The model is presented as in Fig. 6.

Fig. 8. Effects of replacement of Trp218 by tyrosine on inhibition of TEA⁺-induced currents by extracellular and intracellular corticosterone. Mutant rOCT1(C451M,W218Y) was expressed in oocytes and inhibition of TEA⁺-induced currents by corticosterone was measured as in Figs. 2 and 4. For comparison,

inhibition curves obtained under identical experimental conditions in oocytes expressing rOCT1(C451M) are indicated as lines. Data are presented as Fig. 5. They suggest that the affinity for inhibition by extracellular corticosterone was decreased and indicate that maximal inhibition by intracellular corticosterone was decreased when Trp218 was replaced by phenylalanine.

Fig. 9. Effects of replacement of Arg440 by lysine on inhibition of TEA⁺-induced currents by extracellular and intracellular corticosterone. The mutant rOCT1(C451M,R440K) was expressed in oocytes and inhibition of TEA⁺-induced currents by was measured as in Figs. 2 and 4. By this mutation the maximal inhibition by intracellular corticosterone was reduced.

Fig. 10. Effects of replacements of Leu447 by tyrosine and of Phe160 by alanine on inhibition of TEA⁺-induced currents by extracellular TBuA⁺. Mutants rOCT1(C451M,L447Y) and rOCT1(C451M,F160A) were expressed in oocytes. Inhibition of TEA⁺-induced currents by extracellular TBuA⁺ was measured as in Fig. 2. The affinity for extracellular TBuA⁺ was increased by both mutations.

Fig. 11. Docking of TBuA⁺ to the outward-facing substrate cleft of rOCT1. A side view (upper panel) and a view from the extracellular side (lower panel) are shown. The model is presented as in the upper and middle panels of Figs. 6 and 7.

Fig. 12. Sequence alignment of transmembrane helices of OCTs that interact with corticosterone and the corresponding helices of LacY. Amino acids that are conserved between LacY and OCTs are on grey background. Amino acids that are critical for corticosterone interaction with OCT1 are boxed. The amino acids that are

conserved between LacY and OCTs are apparently not involved in corticosterone binding.

TABLE 1

Effects of various mutations in rOCT1 on affinities of corticosterone from the extracellular or intracellular side of the plasma membrane. rOCT1 wildtype or rOCT1 with the indicated mutations were expressed in oocytes. Inhibition of currents induced by superfusion with 0.2 mM or 2 mM TEA⁺ by extracellular or intracellular corticosterone was measured as in Figs. 2 and 4. The Hill equation was fitted to inhibition curves of individual oocytes and IC₅₀ values were calculated. Mean IC₅₀ values \pm S.E.M. are shown. The numbers of measured oocytes are presented in parentheses. The ratios between the mean IC₅₀ values measured with 2 mM TEA⁺ and 0.2 mM TEA⁺ ($f_{(\text{part. comp.})}$) were used to calculate the K_i values from the IC₅₀ value obtained with 0.2 mM TEA⁺. The K_i value in brackets was calculated assuming competitive inhibition.

	Wildtype	C451M	C451M, L447Y	C451M, Q448E	C451M, L447Y Q448E	C451M, F160A	C451M, Y222F	C451M, W218Y	C451M, R440K
Inhibit. from extracell.									
IC ₅₀ (0.2mM TEA)	66 \pm 17 (3)	49 \pm 5 (11)	11 \pm 1.2*** (8)	48 \pm 10 (6)	8.1 \pm 0.8** (4)	13 \pm 1** (5)	101 \pm 7*** (5)	333 \pm 42*** (4)	112 \pm 15*** (6)
IC ₅₀ (2mM TEA)	257 \pm 90 (4)	232 \pm 46 (9)	38 \pm 10 (7)	191 \pm 58 (5)	34 \pm 11 (8)	32 \pm 8 (3)	417 \pm 174 (5)	Not determined Max. Inhibit. decreased (3)	588 \pm 124* (4)
f (part. comp.)	3.89	4.73	3.45	3.98	4.20	2.50**	4.13		4.63
K_i	27.8 \pm 7.2	18.4 \pm 1.9	5 \pm 0.5***	20 \pm 4.2	3.3 \pm 0.3**	6.9 \pm 1.8*	26.2 \pm 1.7	(93.3 \pm 11.8)***	40.4 \pm 5.3**
Inhibit. from intracell.									
IC ₅₀ (0.2mM TEA)		132 \pm 34 (5)	28 \pm 4* (4)	4.6 \pm 0.7** (5)		32 \pm 8* (4)	183 \pm 41 (3)	Not determined Max. Inhibit. decreased (5)	124 \pm 33 (5)
IC ₅₀ (2mM TEA)	335 \pm 13 (3)	315 \pm 58 (7)	25 \pm 3** (6)	9.2 \pm 1.8** (4)		78 \pm 20* (4)	502 \pm 108 (5)	Not determined Max. Inhibit. decreased (4)	Not determined Max. Inhibit. decreased (5)
f (part. comp.)		2.63	0.89**	2.00		2.44	2.74		
K_i		71 \pm 19 ^{○○○}	28 \pm 4*, ^{○○○}	2.7 \pm 0.4**, ^{○○○}		18 \pm 4*, ^{○○○}	69 \pm 15 ^{○○○}		

*P<0.05, **P<0.01, ***P<0.001, ANOVA with Tukey test, difference compared with rOCT1(C451M); **P<0.01, Student's t-test, difference to rOCT1(C451M); ^{○○○}P<0.001, Student's t-test, difference to inhibition from extracellular

TABLE 2

Effect of mutations that change the interaction of corticosterone with rOCT1 on the affinity of MPP⁺. Inhibition of [¹⁴C]TEA⁺ uptake by MPP⁺ was measured in oocytes expressing wildtype rOCT1 or rOCT1 mutants. Oocytes were incubated 15 min with 5 μM [¹⁴C]TEA⁺ in the presence of eight different concentrations of MPP⁺. IC_{50(MPP)} values of individual experiments were determined by fitting the Michaelis Menten equation to the data. Mean values ± SEM are presented. Numbers of independent experiments are indicated in parenthesis.

	IC _{50(MPP)}
Wildtype	7.4 ± 1.1 (3)
C451M	9.4 ± 1.3 (4)
C451M, L447Y	0.46 ± 0.09** (3)
C451M, Q448E	2.5 ± 0.52* (3)
C451M, L447Y, 448E	0.31 ± 0.05** (3)
C451M, F160A	19.5 ± 2.0** (3)
C451M, W218Y	23.1 ± 2.2*** (3)
C451M, R440K	18.6 ± 2.2** (3)

*P<0.05, **P<0.01, ***P<0.001, significance for difference compared to rOCT1(C451M) mutant calculated by ANOVA with post hoc Tukey test

TABLE 3

Effects of mutations that change the interaction of corticosterone with rOCT1 on the affinity of TBuA⁺ from extracellular. rOCT1 wildtype or rOCT1 mutants were expressed in oocytes. Inhibition of currents induced by superfusion with 0.2 mM or 2 mM TEA⁺ by extracellular TBuA⁺ was measured as in Fig. 2. The Hill equation was fitted to inhibition curves of individual oocytes and IC₅₀ values were calculated. The data are presented and the K_i values were calculated as in Table 1.

Inhibit.from extracell.	C451M	C451M,F160A	C451M,L447Y	C451M,W218Y	C451M,R440K
IC ₅₀ (0.2mM TEA)	11.8 ± 3.6 (6)	1.2 ± 0.2 (5) ^{***}	1.1 ± 0.3 (5) ^{***}	11.0 ± 0.1 (3)	9.7 ± 2.1 (6)
IC ₅₀ (2mM TEA)	81.5 ± 10.5 (4)	19.3 ± 1.7 (6) ^{***}	6.4 ± 1.7 (5) ^{***}	88.3 ± 14.4 (4)	82.9 ± 16.2 (4)
f (part. comp.)	6.9	15.8 ^{**}	5.8	8.0	8.5
K _i	3.5 ± 1.1	0.18 ± 0.03 ^{***}	0.30 ± 0.08 ^{***}	2.89 ± 0.03	2.43 ± 0.53

^{***}P<0.001, ANOVA with Tukey test, difference compared with rOCT1(C451M); ^{**}P<0.01, Student's t-test, difference to rOCT1(C451M)

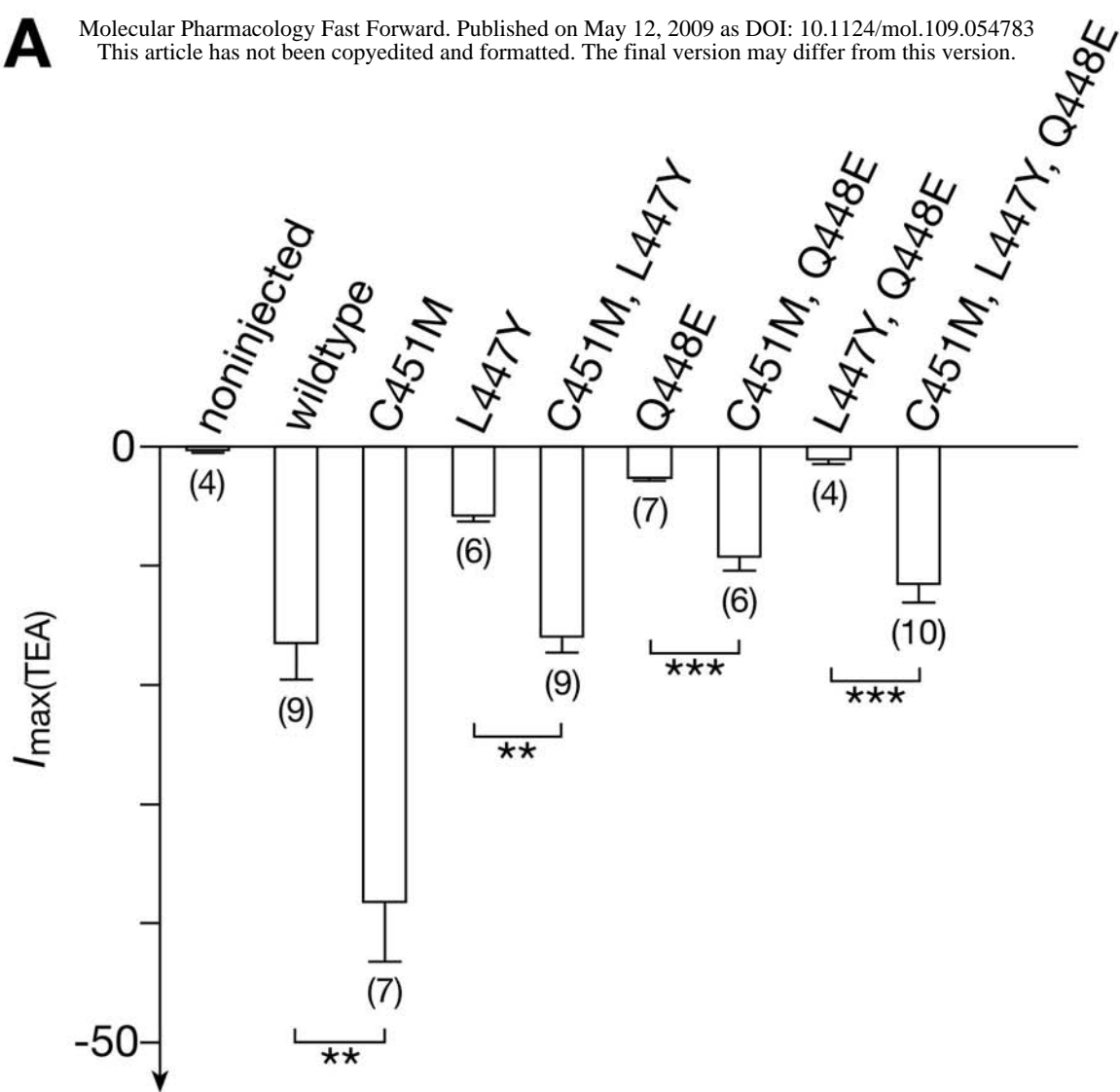
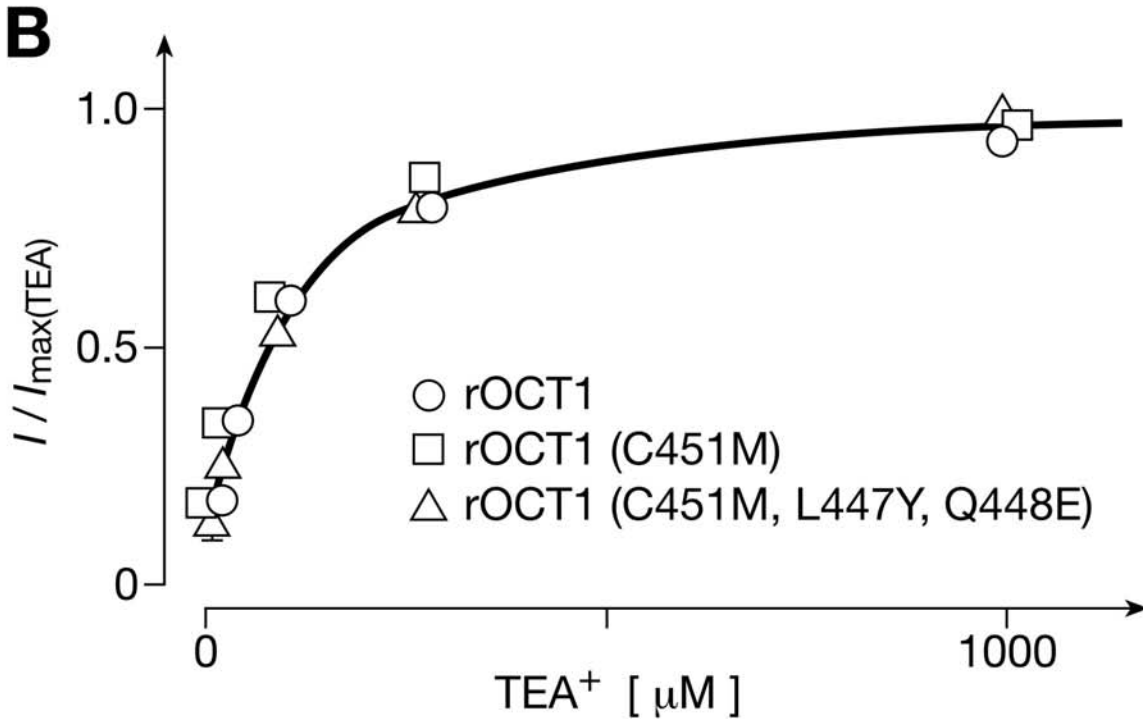
A**B**

Fig. 1

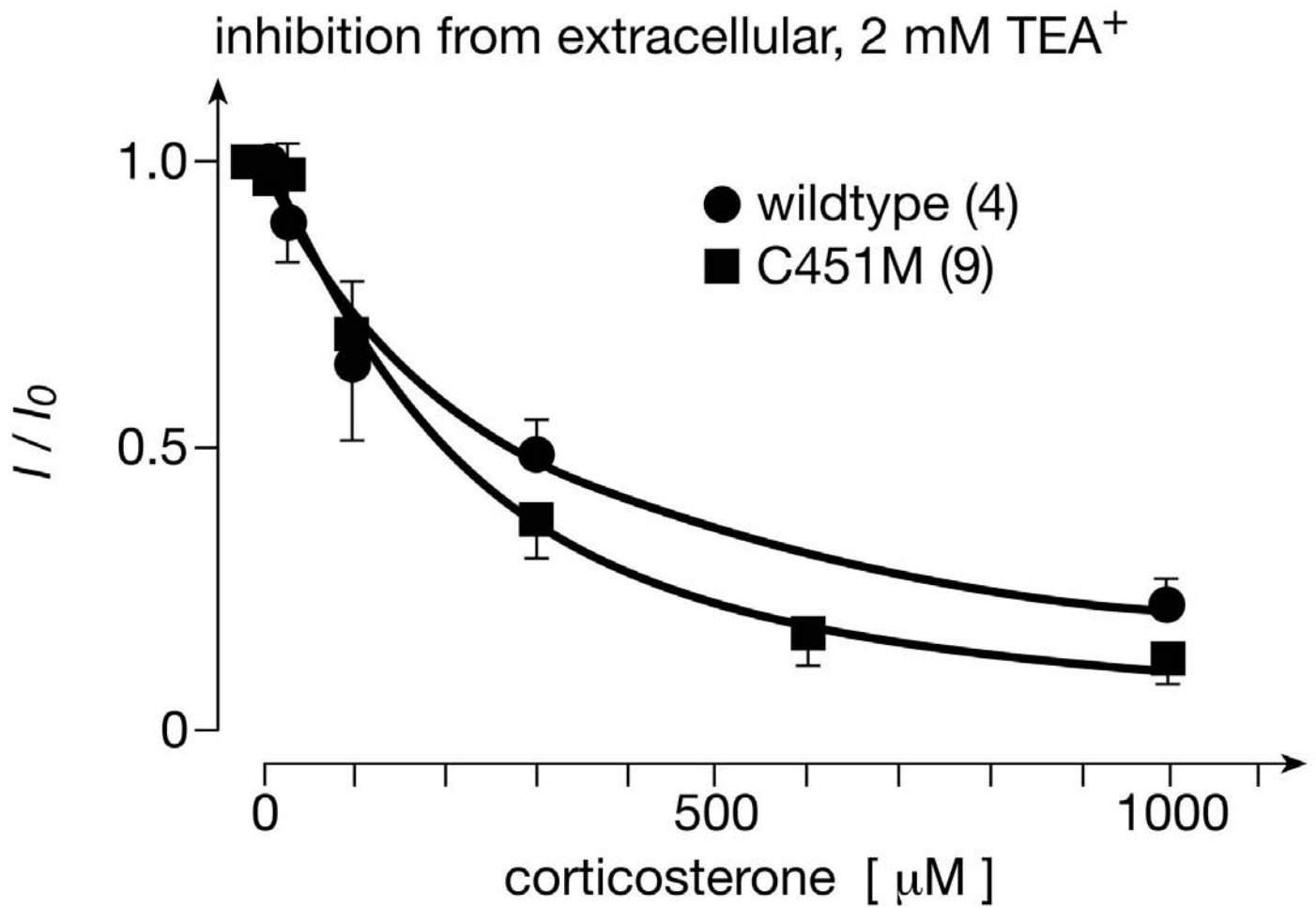
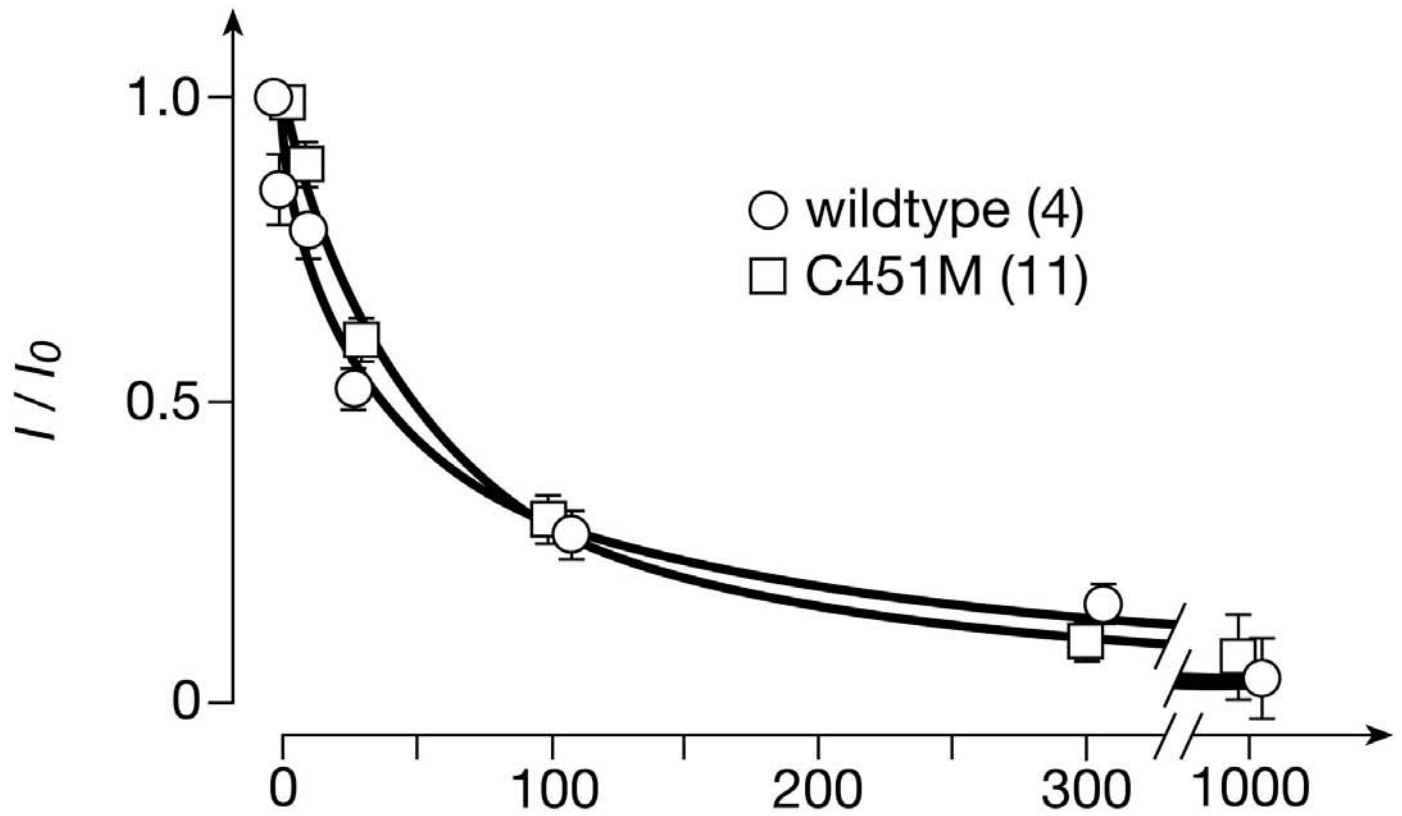


Fig. 2

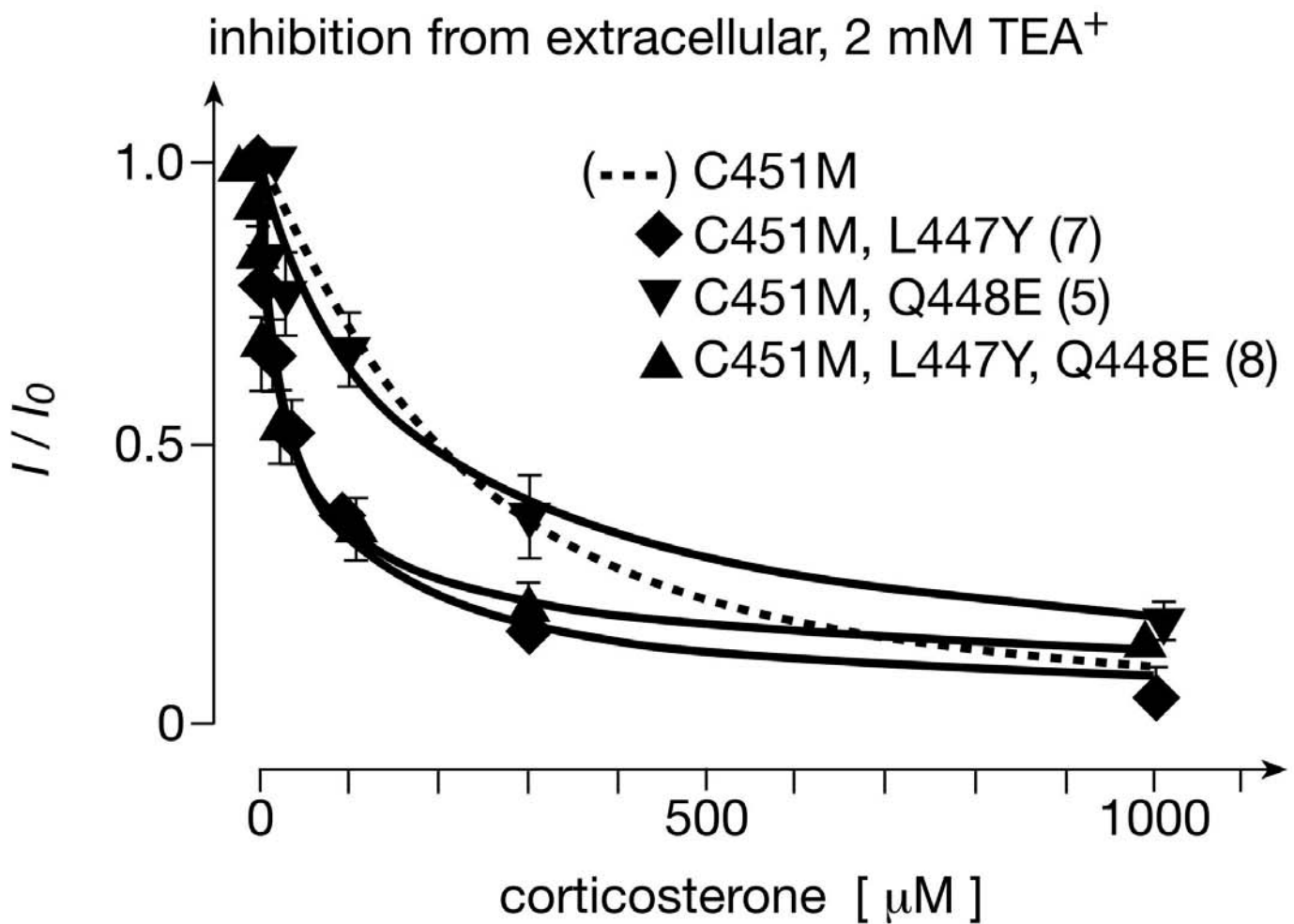
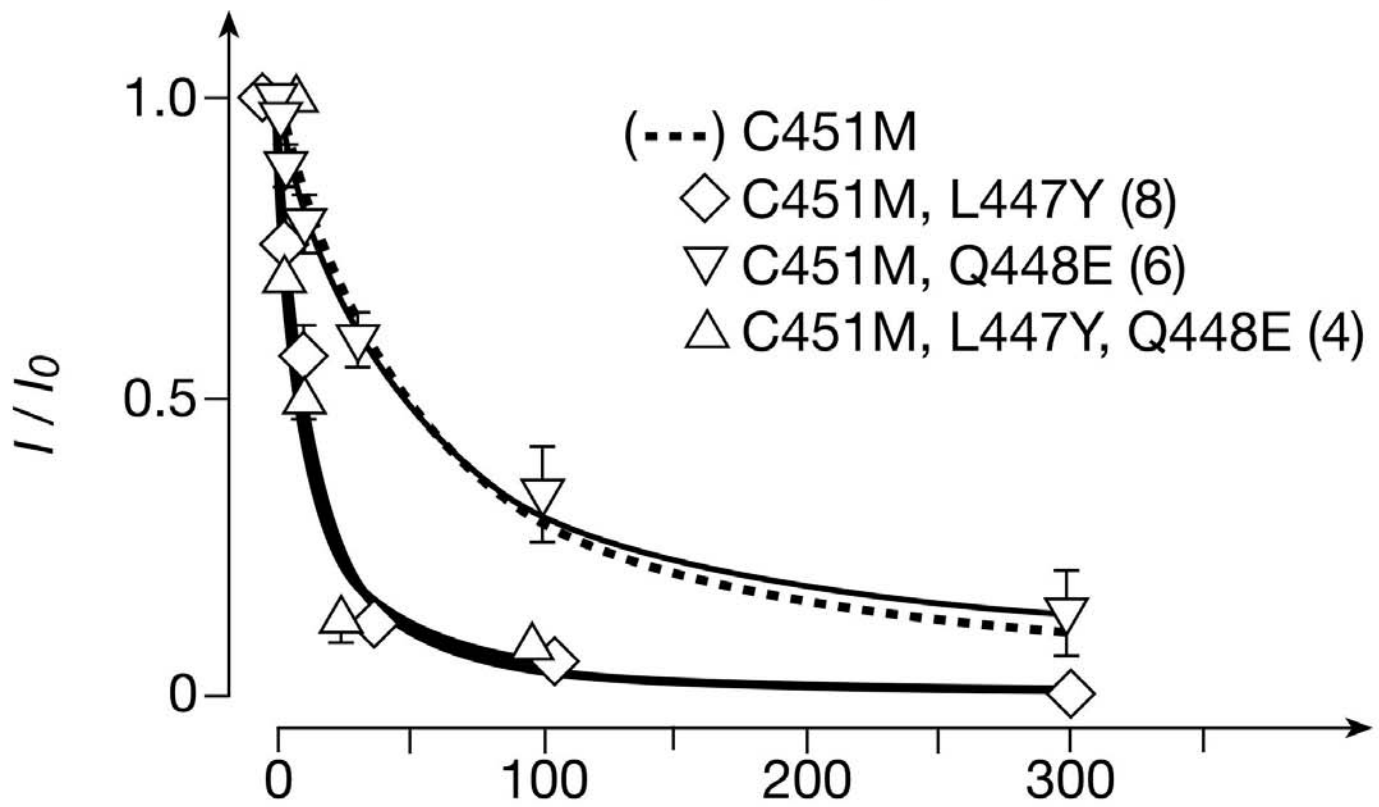


Fig. 3

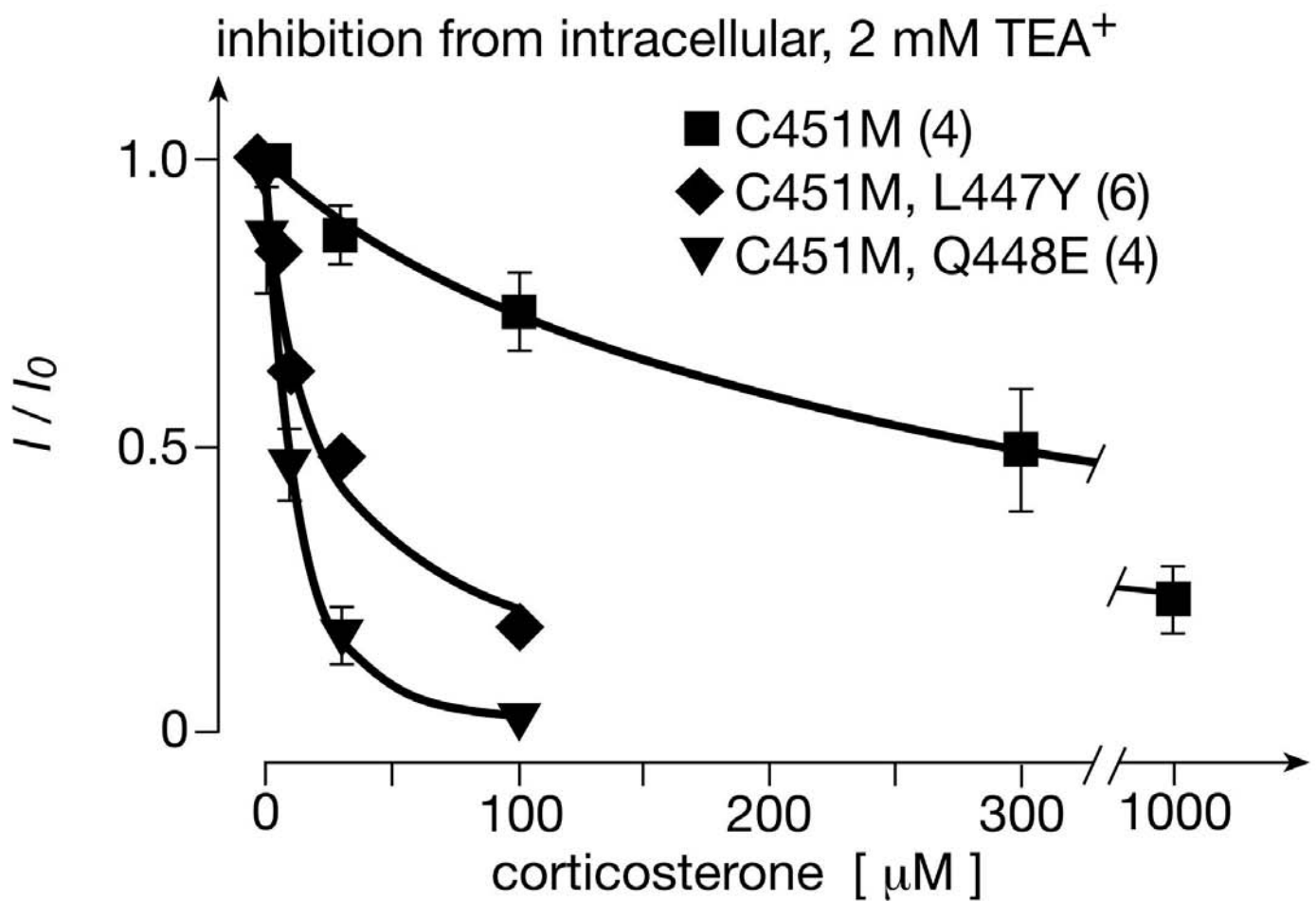
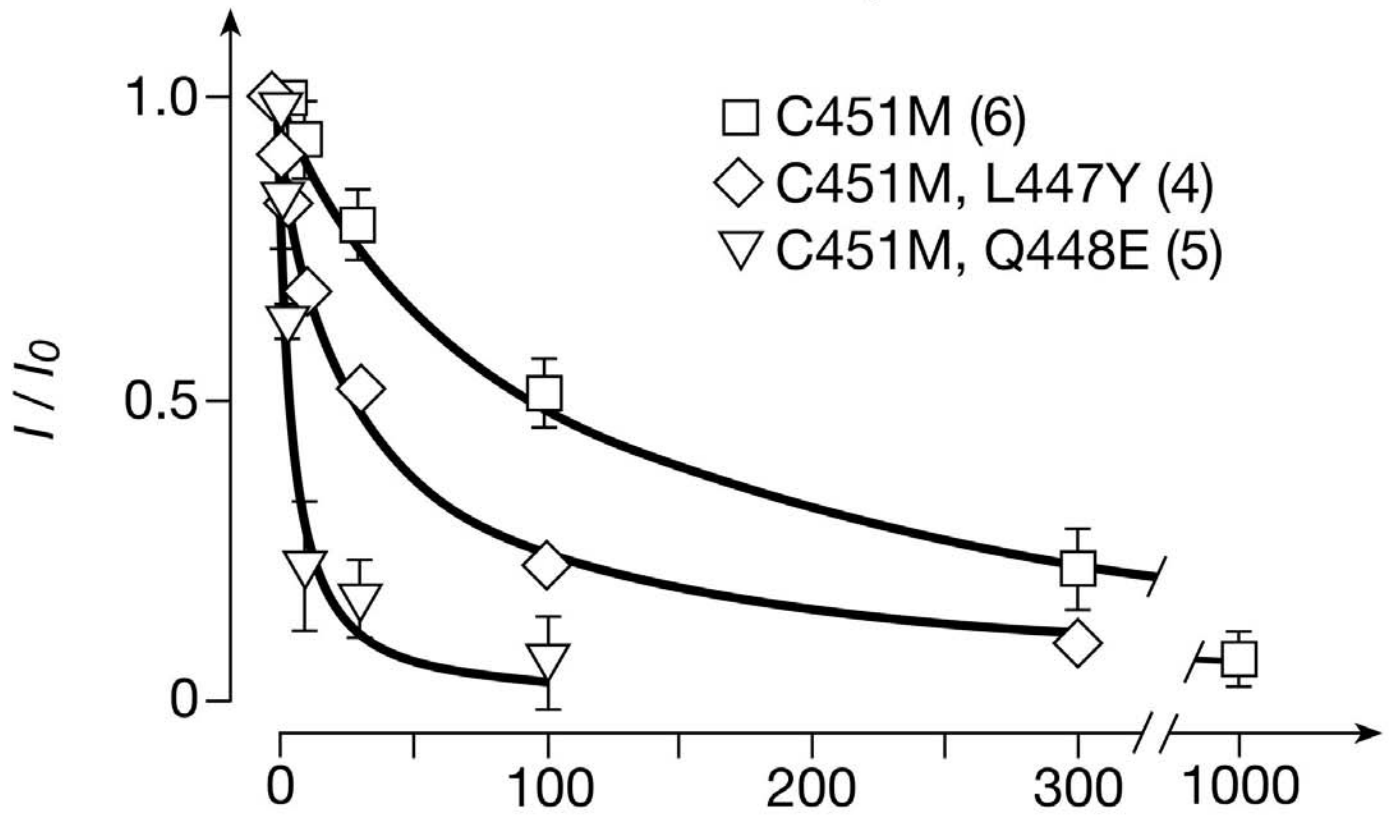


Fig. 4

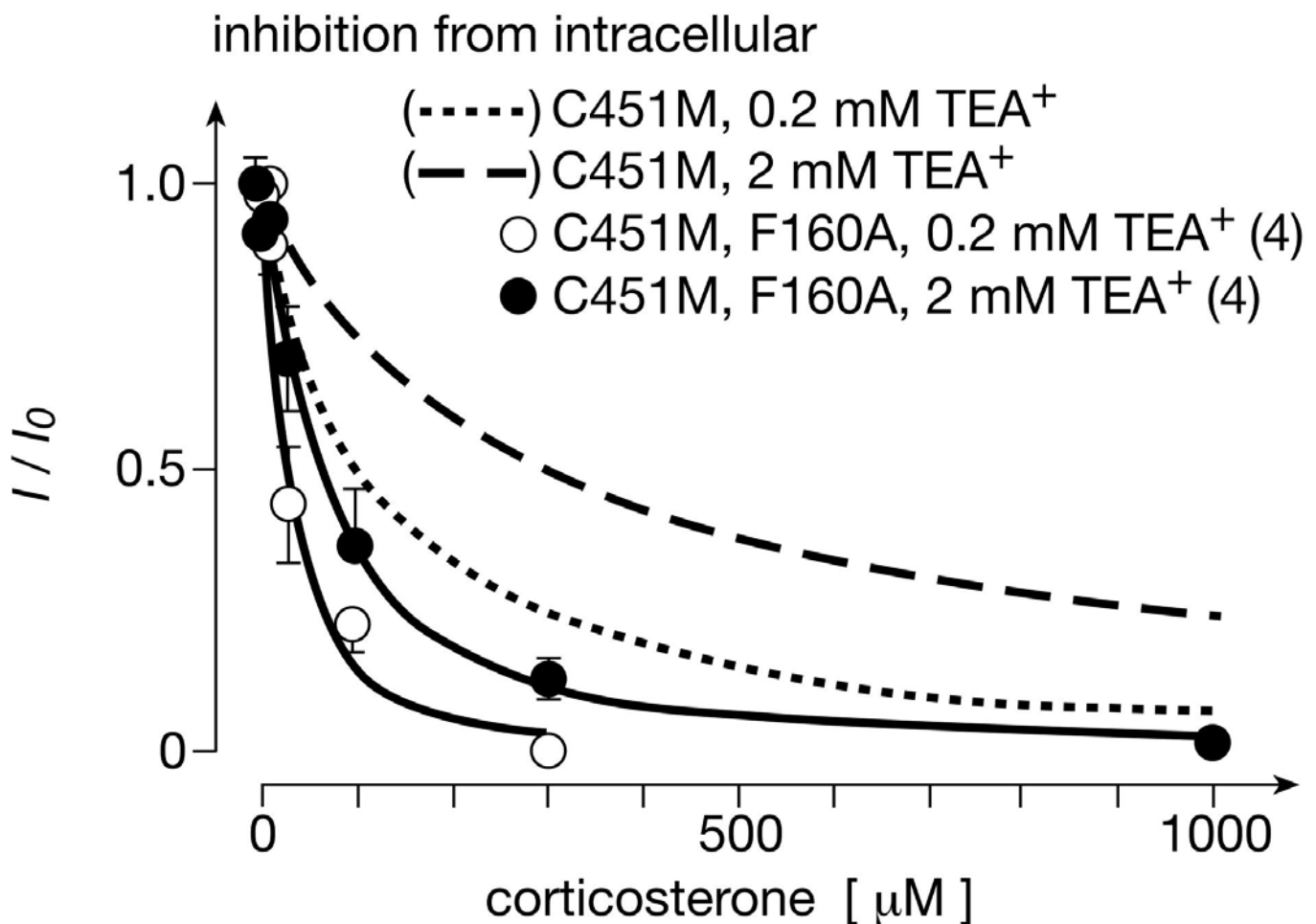
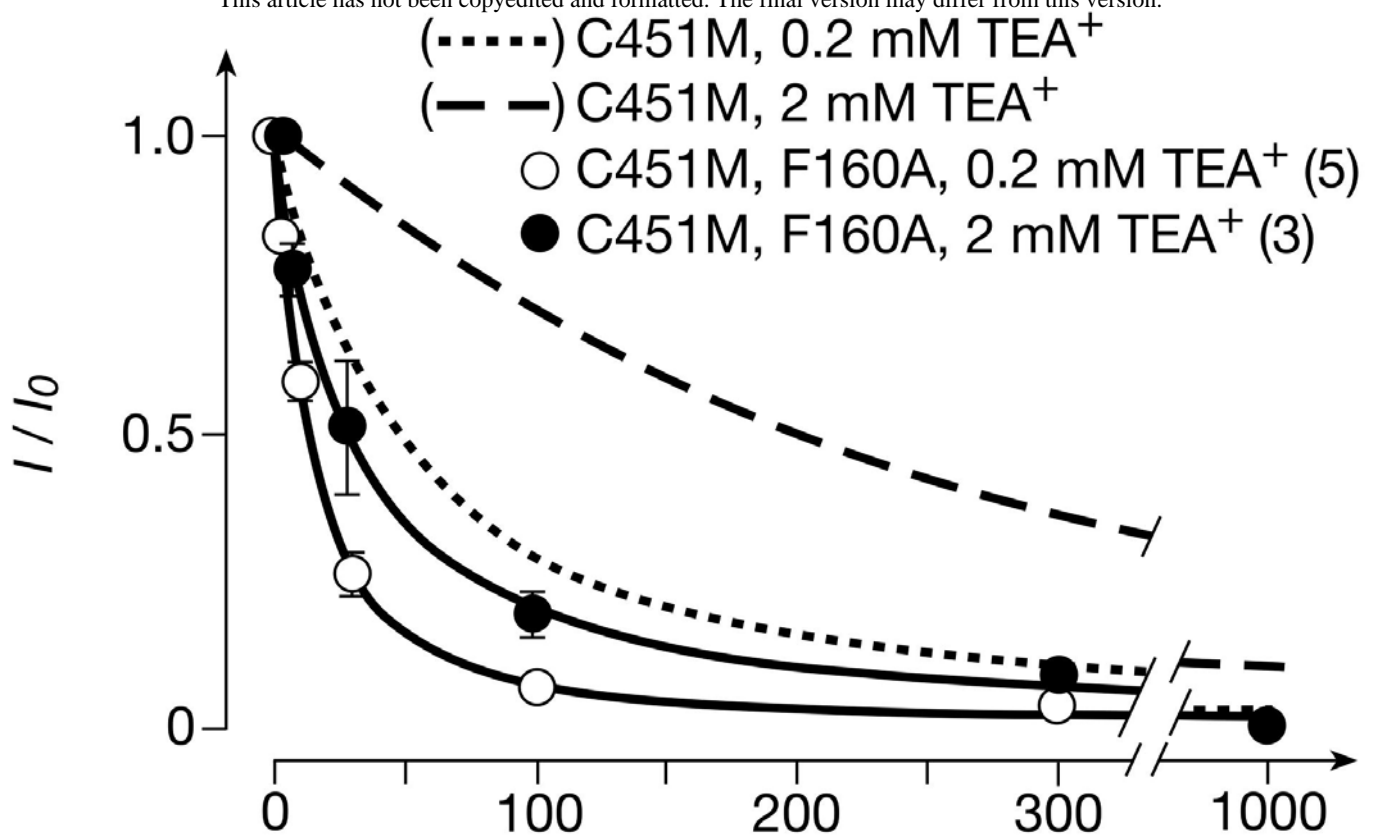


Fig. 5

1 2 3 4 6 8 9 10 11 12

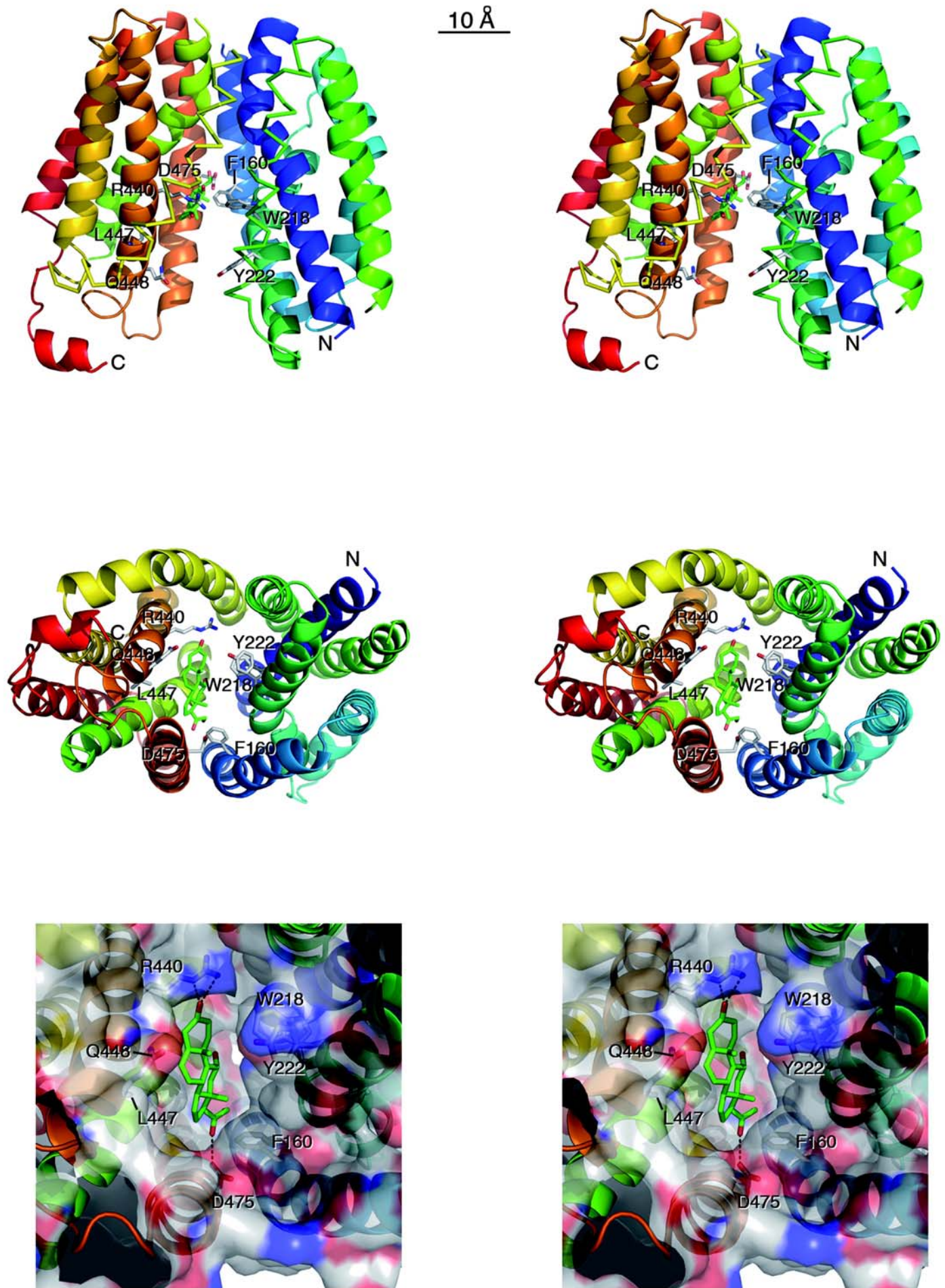


Fig. 6

TMH 1 2 3 4 6 8 9 10 11 12

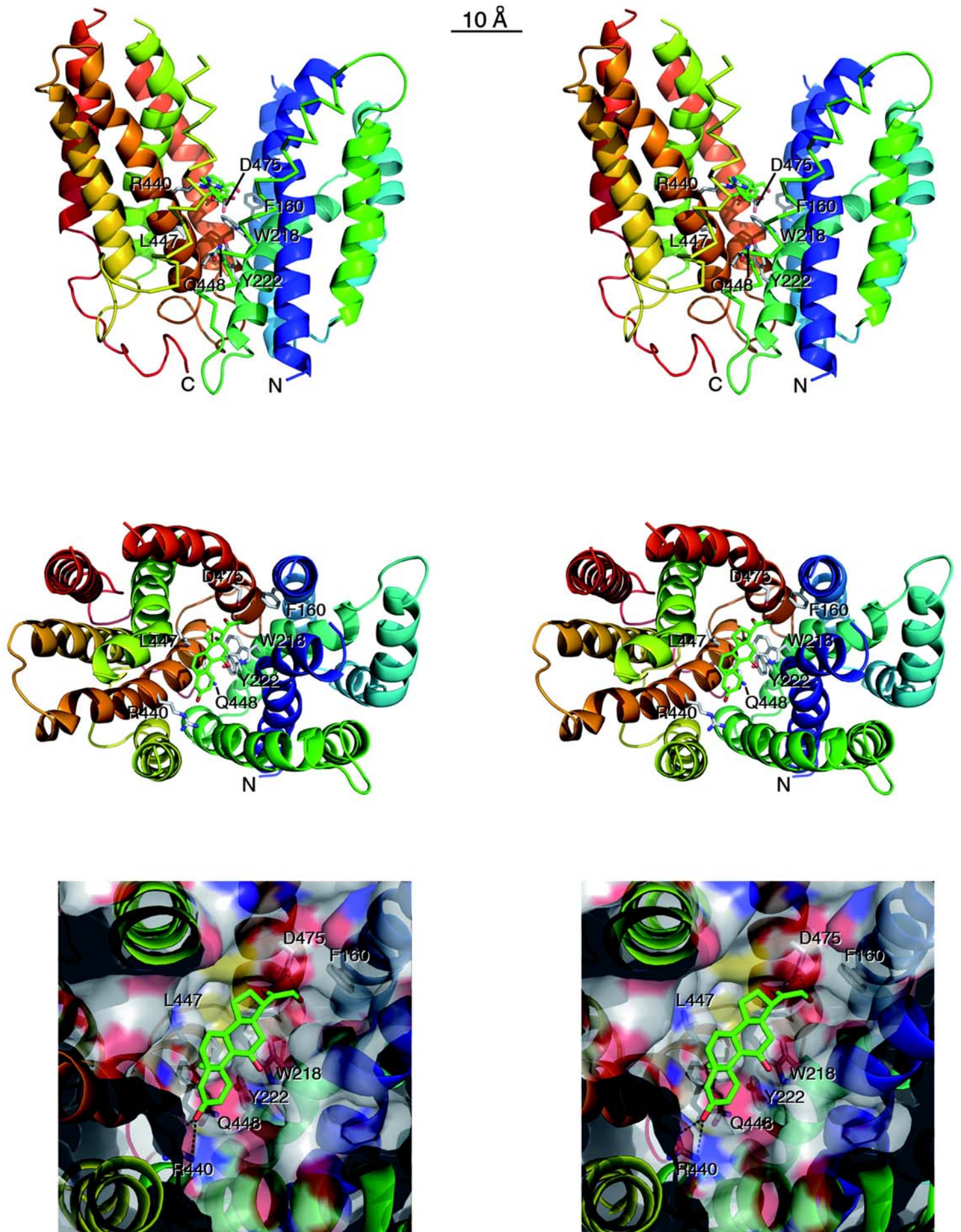


Fig. 7

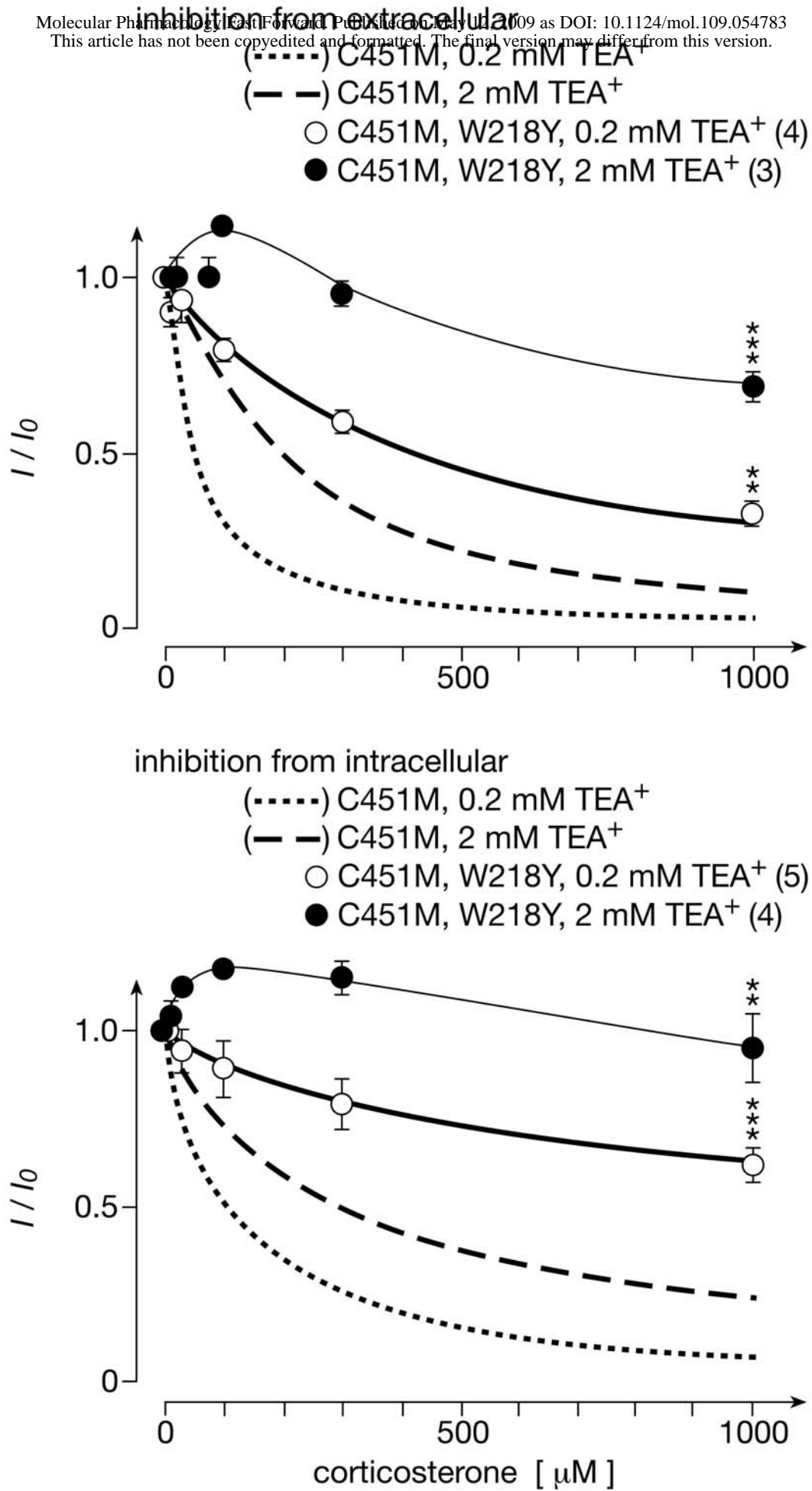


Fig. 8

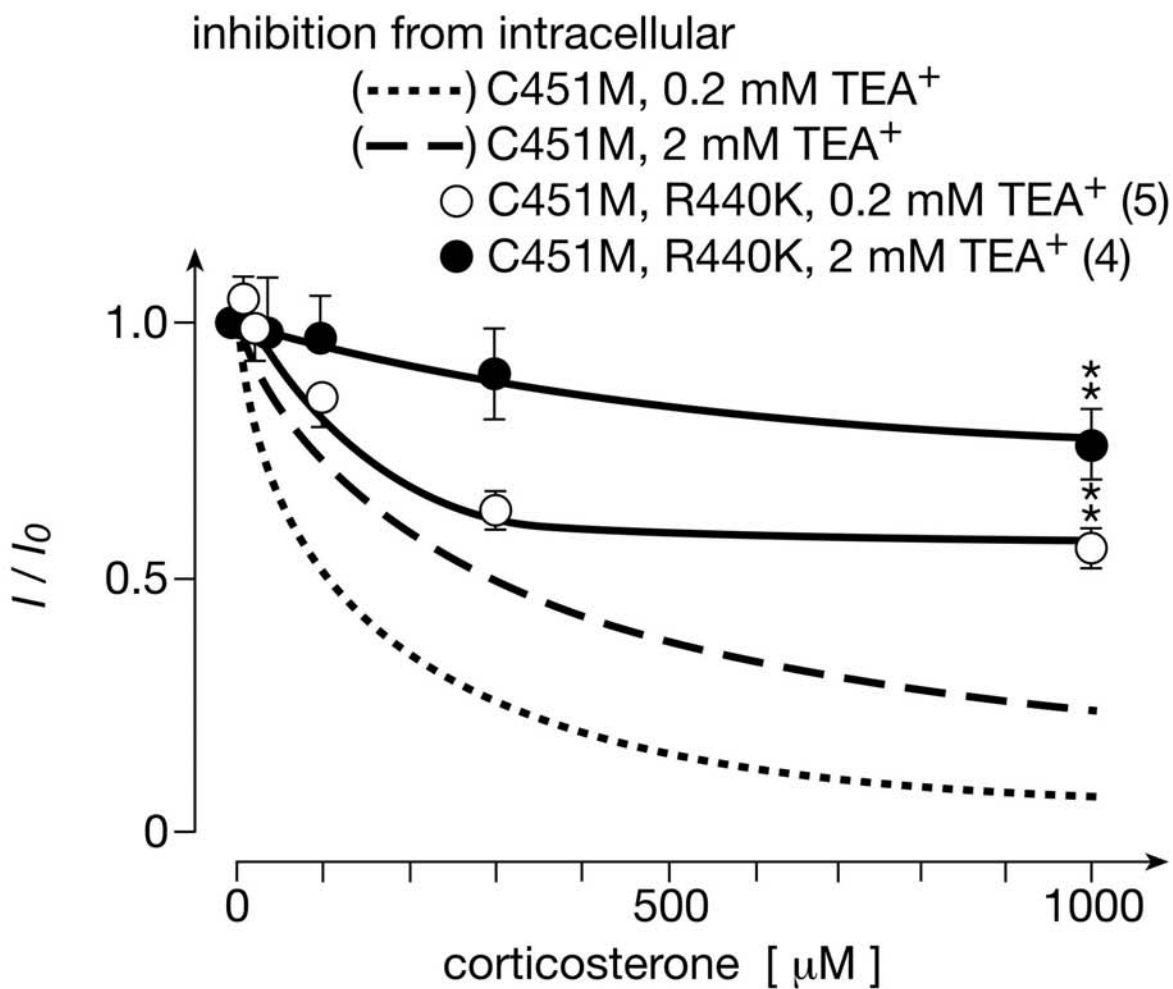
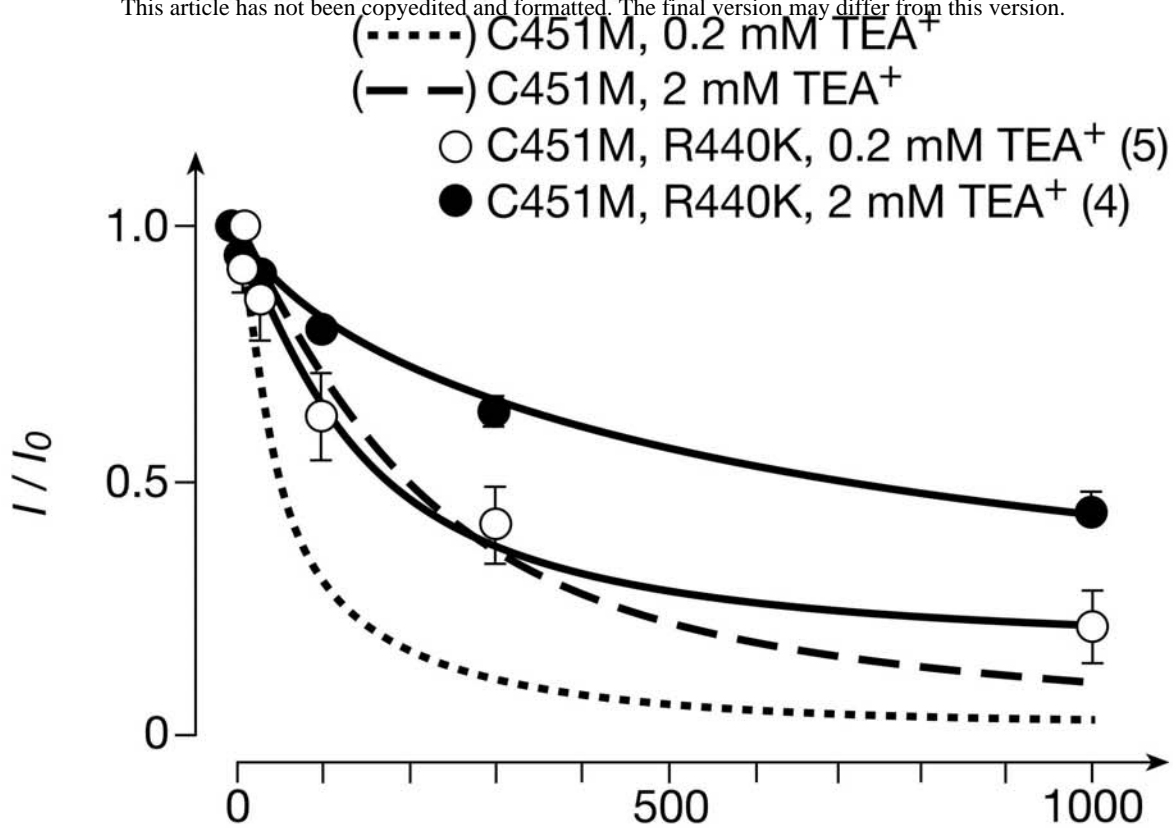


Fig. 9

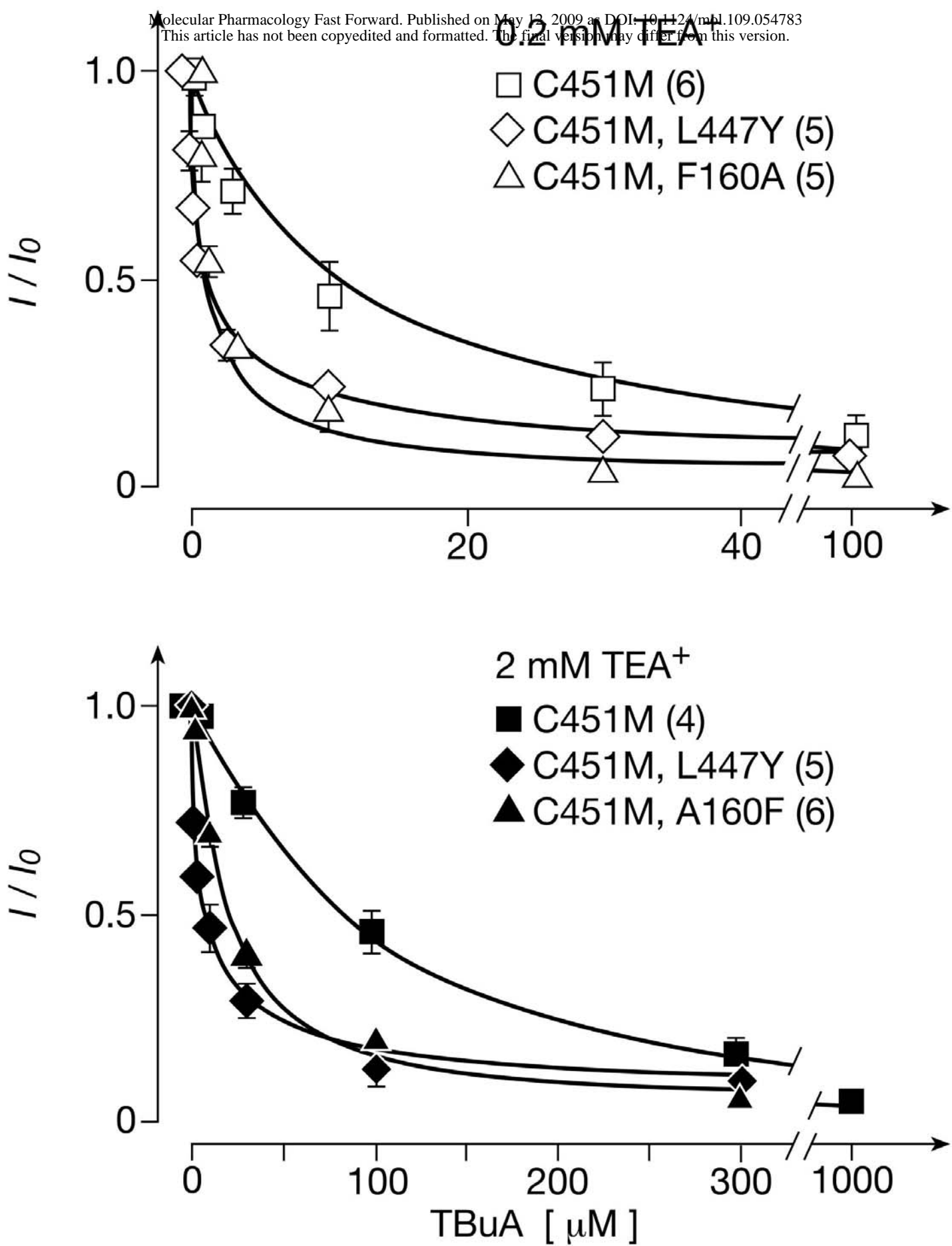


Fig. 10

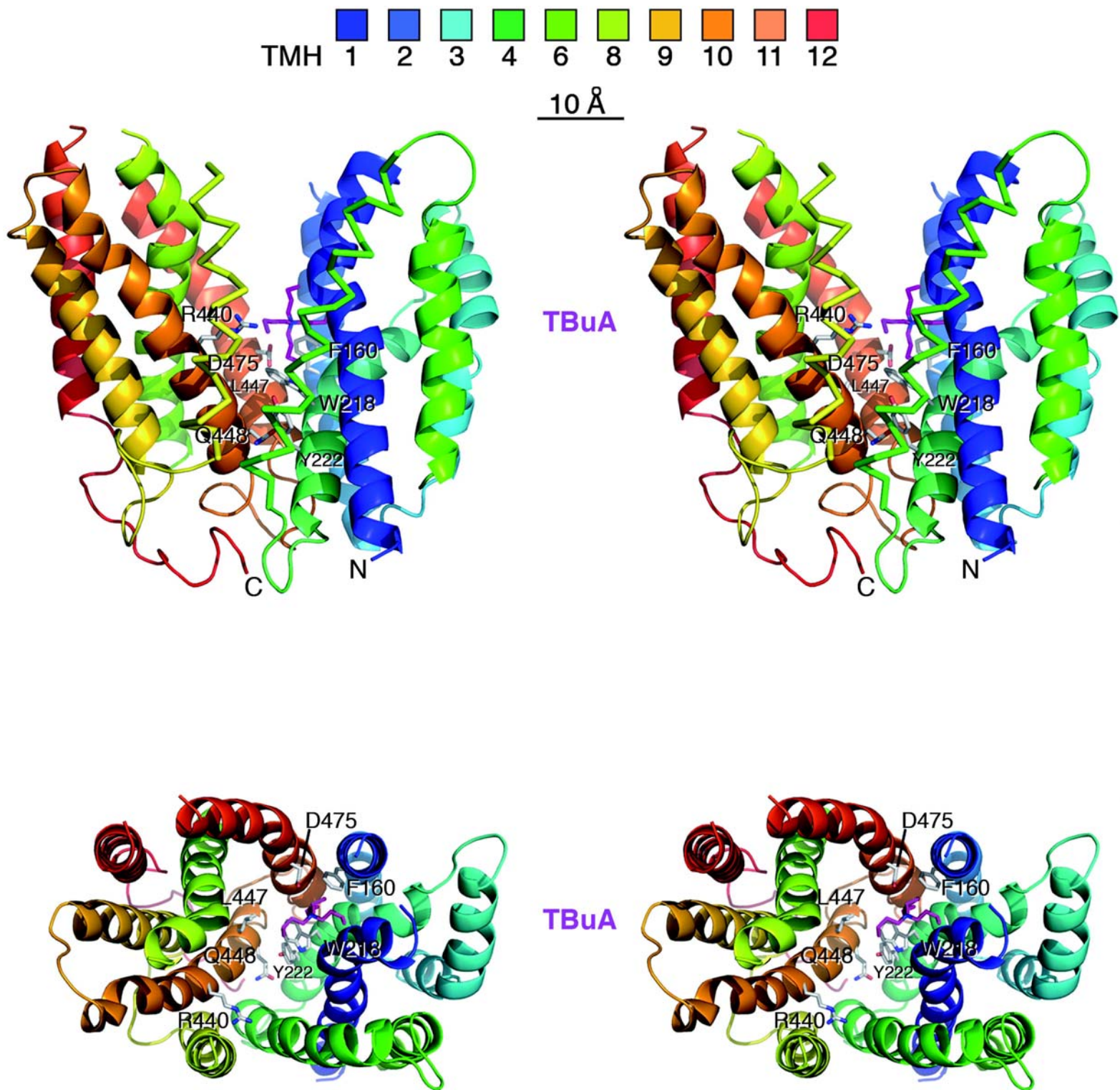


Fig. 11

TMH2 146 173
 rOCT1 AWKVDLFQSCVNLGFFFLGSLVVG^{F169}YIADR
 rOCT2 SWMLDLFQSVVNVGFFFIGAMMIGYLADR
 rOCT3 AWMLDLTQAILNLGFLAGAF^{F169}TLGYAADR
 hOCT3 AWMLDLTQAILNLGELTGAFTLGYAADR
 LacY KSDTGIIFAAISLFSLLFQPLFGLLSDK

TMH4 210 231
 rOCT1 QGMVSKGSWVSGYTLITEFVG-S
 rOCT2 QGLVSKAGW^{W218}LIGYILITEFVG-L
 rOCT3 QGVFGKGAWMTCFVIVTEIVG-S
 hOCT3 QGVFGKGTW^{W218}MTCYVIVTEIVG-S
 LacY LGFCFNAGAPAVEAFIEKVSRRS

TMH10 427 451
 rOCT1 ELH-WLNVTLACLGRMGATIVLQ^{R440}MVC
 rOCT2 DLQ-WLKITIAACLGRMGITMAYEMVC
 rOCT3 GIP-WLRTTVATLGRLGITMAFEIVY
 hOCT3 GIA-WLRTTVATLGRLGITMAFEIVY
 LacY ALEVVILKTLHMFEVFP^{L447 Q448}LLVGCFKYI

TMH11 461 492
 rOCT1 FIRNLGMMVCSALCDLGGI^{D475}FTPFMVFRLMEVW
 rOCT2 YIRNLGVLVCSSMODIGGIITPFLVYRLTDIW
 rOCT3 TLRNFGVSLCSGLCDFGGIIAPFLLFRLAAIW
 hOCT3 TLRNFGVSLCSGLCDFGGIIAPFLLFRLAAVW
 LacY FSATIYLVCF^{D475}CFKQLAMIFMSVLAGNMYESI

Fig. 12